




 Cite this: *RSC Adv.*, 2022, **12**, 18864

# A review of the catalytic conversion of glycerol to lactic acid in the presence of aqueous base

 Doğan Akbulut <sup>a</sup> and Saim Özkar <sup>\*b</sup>

Lactic acid is a high-value-added chemical with large production, which is used in many industries including the production of pyruvic and acrylic acids. Lactic acid is largely obtained from the oxidation of glycerol, which is a prevalent by-product of biodiesel production. However, the oxidation of glycerol to lactic acid requires harsh reaction conditions such as high temperature and pressure as well as the use of a hefty strong base. In the presence of suitable catalysts, the production of lactic acid from glycerol can be achieved under mild conditions with 1 equivalent base per mole of glycerol. Herein, we review the reports of the catalytic conversion of glycerol to lactic acid in an aqueous alkaline medium considering the reaction conditions, catalytic activity for glycerol conversion and selectivity for lactic acid. We start first with the reports on the use of homogeneous catalysts that have high catalytic activity but miserable recovery. Next, we discuss the employment of colloidal metal(0) nanoparticles as catalysts in glycerol oxidation. The papers on the use of supported metal(0) nanoparticles are reviewed according to the type of support. We then review the polymetallic and metal/metal oxide nanocatalysts used for the conversion of glycerol to lactic acid in an alkaline medium. The catalysts tested for glycerol conversion to lactic acid without any additional bases are also discussed to emphasize the importance of a strong base for catalytic performance. The proposed mechanisms of glycerol oxidation to lactic acid in the presence or absence of catalysts as well as for the formation of side products are discussed. The available experimental kinetics data are shown to fit the mechanism with the formation of glyceraldehyde from glycerol alkoxide as the rate-determining step.

 Received 16th May 2022  
 Accepted 14th June 2022

DOI: 10.1039/d2ra03085c

[rsc.li/rsc-advances](http://rsc.li/rsc-advances)
<sup>a</sup>Department of Chemistry, Middle East Technical University, Ankara, Turkey. E-mail: [dogan.akbulut@metu.edu.tr](mailto:dogan.akbulut@metu.edu.tr)
<sup>b</sup>Department of Chemistry, Middle East Technical University, Ankara, Turkey. E-mail: [sozkar@metu.edu.tr](mailto:sozkar@metu.edu.tr)

## 1. Introduction

Lactic acid (2-hydroxypropanoic acid, LA) is an extensively used chemical in a wide range of industrial applications including foods,<sup>1</sup> drugs,<sup>2</sup> cosmetics,<sup>3</sup> medication,<sup>4</sup> and the production of



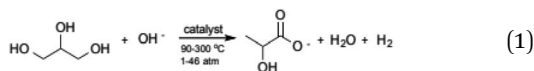
*Doğan Akbulut graduated from the Chemistry Department, Middle East Technical University in 2020. Currently, he is a graduate student and research assistant at the same department working in the field of organic chemistry under the supervision of Assoc. Prof. Dr Serhan Turkyilmaz.*



*Özkar graduated from the Istanbul Technical University in 1972, received PhD at Technical University of Munich in 1976, joined METU in 1979, became Full Professor in 1988, spent one year at Max Planck Institute in Mülheim in 1986, 2 years at University of Toronto in 1988, 5 years at Colorado State University since 2000, and initially worked on organometallics and metal carbonyls for converting them into new materials. He has 22 years of experience in metal nanoparticles. He was awarded 1996 Science Prize by Scientific and Technological Research Council of Turkey, and has been member of Turkish Academy of Sciences since 1996.*



chemicals such as pyruvic acid,<sup>5</sup> acrylic acid,<sup>6</sup> propionic acid,<sup>7,8</sup> acetaldehyde,<sup>9</sup> alanine,<sup>10</sup> and glycerol carbonate.<sup>11</sup> It has also been used to remove hyperpigmentation<sup>12</sup> and to extend the shelf life of foods.<sup>13</sup> LA can be produced on a large scale starting with glycerol, which is a waste product of the continuously increasing biodiesel production through biomass conversion.<sup>14–17</sup> However, the conversion of glycerol to LA requires high temperatures and pressures as well as the use of a large amount of base as the reaction occurs in an alkaline medium (eqn (1)).



Fortunately, it has been shown that performing the transformation in the presence of suitable catalysts reduces the amount of base and increases the conversion even under milder conditions.<sup>18</sup> Since the reaction in eqn (1) is accompanied by the formation of many side products such as glyceraldehyde (GAL), glyceric acid (GA), ethylene glycol (EG), 1,2-propanediol (PDO), pyruvaldehyde (PAL), formic acid (FA), oxalic acid (OA), and acetic acid (AA),<sup>19</sup> the big challenge in the production of LA from glycerol is the development of catalysts, which also provides high selectivity for LA in addition to the high activity. It is also noteworthy that the catalyst is anticipated to retain high catalytic performance even when starting with the crude glycerol obtained from the biodiesel industry.

Herein, we review all the papers reporting the catalytic oxidation of glycerol to LA by considering the catalytic activity for glycerol conversion, selectivity for LA, stability/durability, recyclability/reusability, and ultimately the overall catalytic efficacy. The reaction parameters such as temperature, pressure, amount of required base, reaction time, and catalyst composition are considered to make a rational comparison of all the catalysts that were tested for the glycerol conversion to LA and the results are critically discussed. The catalysts tested under base-free conditions for the selective glycerol conversion to LA will also be briefly considered to indicate the effect of using a base on the activity of the catalysts and reaction conditions with glycerol conversion and the selectivity for LA. The mechanisms of the catalytic transformation of glycerol to LA will be discussed as far as the available knowledge on the structure of intermediates and transition states, kinetics data and other findings allow. This review ends with a Conclusion section that also includes our suggestions for future research in the field.

Our review of the catalysts reported for the conversion of glycerol to LA is in the following order: (i) homogeneous catalysts obtained starting with the water-soluble complexes of transition metal ions, particularly, iridium(i) and ruthenium(ii) ions, (ii) monometallic or bimetallic colloidal nanoparticles of transition metals usually stabilized by water-soluble polymers, (iii) transition metal nanoparticles supported on the surface of metal oxides, (iv) polymetallic nanoparticles supported on the metal oxides, (v) metal/metal oxide nanoparticles, (vi) transition metal nanoparticles supported on the surface of carbonaceous materials, (vii) other heterogeneous catalysts. We will also

briefly review the catalysts used without an additional base for glycerol conversion to LA to emphasize the importance of base for the reaction.

## 2. Homogeneous catalysts in the conversion of glycerol to LA

There exist four papers reporting the use of iridium complexes for the glycerol conversion to LA.<sup>20–23</sup> The first paper by Crabtree *et al.*<sup>20</sup> reports the testing of ten  $(\eta^5\text{-C}_5\text{Me}_5)\text{Ir}^{\text{III}}$  complexes as homogeneous catalysts in the conversion of glycerol to LA in an alkaline medium. These complexes have higher activity for glycerol conversion and selectivity for LA formation than the previously reported heterogeneous systems. Additionally, COD (1,5-cyclooctadiene) and dicarbonyliridium(i) complexes bearing two IMe (1,3-dimethylimidazol-2-ylidene) ligands were tested as homogeneous catalysts in the same reaction, whereby  $[(\text{CO})_2\text{Ir}(\text{IME})_2]\text{BF}_4$  shows two-fold higher catalytic activity than  $[(\text{COD})\text{Ir}(\text{IME})_2]\text{BF}_4$ .<sup>20</sup> Among the tested complexes,  $[\text{Cp}^*\text{Ir}(\text{IME})_2\text{Cl}]\text{BF}_4$  provides the highest catalytic activity (TOF =  $317 \text{ h}^{-1}$ ) and selectivity (>95%) for the formation of LA from glycerol in alkaline solution at  $160 \text{ }^\circ\text{C}$  (Table 1).<sup>20</sup> The catalytic activities of the iridium complexes reported in that paper<sup>20</sup> are quite low compared to that of other homogeneous catalysts reported for the conversion of glycerol to LA (*vide infra*). An important observation is the insensitivity of reactions catalysed by  $[\text{Cp}^*\text{Ir}(\text{IME})_2\text{Cl}]\text{BF}_4$  and  $(\text{CO})_2\text{Ir}(\text{IME})_2\text{BF}_4$  to air, so that the reaction does not require an inert atmosphere.<sup>20</sup> On the other hand, a dramatic decrease in catalytic activity was observed for  $[\text{Ir}(\text{COD})(\text{IME})_2]\text{BF}_4$  when the reaction was performed in air. Unexpectedly, no information about the reusability and recovery of catalysts has been reported in that paper.<sup>20</sup> High equivalent base per mole of glycerol was required for achieving selectivity higher than 95%.<sup>20</sup> The increase in the amount of base necessitates additional water to minimize the solubility problem. Potassium hydroxide was found to provide the highest performance, most likely due to high solubility. Since the reactions are carried out in a basic solution, the target product is expected to be the lactate salt instead of the protonated form as given in Fig. 3 of that paper.<sup>20</sup>

The second paper, by Williams *et al.*,<sup>21</sup> reports the use of five iridium complexes containing COD and bidentate py-IME (methylpyridylimidazol-2-ylidene) or py-IMes (mesitylene-pyridylimidazol-2-ylidene) ligands as homogeneous catalysts for the conversion of glycerol to LA in an alkaline medium. The iridium complex containing COD and (pyridyl)carbene ligands shows the highest catalytic activity (TOF =  $6 \times 10^3 \text{ h}^{-1}$ ) and selectivity (>99%) ever reported for this conversion at  $145 \text{ }^\circ\text{C}$  (Table 1). Pyridylcarbene ligand in the complex is expected to prevent ligand scrambling in the complexes.<sup>20</sup> No side products were observed in the reactions catalysed by  $[\text{Ir}(\text{COD})(\text{py-IMes})]\text{OTf}$  giving a selectivity higher than 95%. Substitution of COD by two CO ligands in  $[\text{Ir}(\text{COD})(\text{py-IMes})]\text{OTf}$  causes a notable lowering in the catalytic activity.<sup>21</sup> After approximately 25% conversion of glycerol to lactate salt, a decrease was observed in



Table 1 The parameters and results of the catalytic conversion of glycerol to LA in a basic medium by using homogeneous catalysts<sup>a</sup>

Catalysts	Base (equiv.)	TOF (h <sup>-1</sup> )	Time (h)	T (°C)	Select. (%)	Conv. (%)	Ref.
[Cp*Ir(IME) <sub>2</sub> Cl] <sup>+</sup> BF <sub>4</sub> <sup>-</sup>	0.58	317 <sup>a</sup>	15	160	>95	34.8	20
[Ir(COD)(py-IME)]OTf	1	6 × 10 <sup>3a</sup>	768	145	>99	45.6	21
[[ <sup>Bim</sup> 2NNNRuCl(PPh <sub>3</sub> ) <sub>2</sub> ]Cl]	1	312 <sup>a</sup>	48	140	98	46	22
Na <sup>+</sup> [Ir(NHC-ph-SO <sub>3</sub> ) <sub>2</sub> (CO) <sub>2</sub> ] <sup>-</sup>	1	4.3 × 10 <sup>4</sup>	8	140	100	92	23
NaOH	0.18	—	3.7	300	88.2	93	24

<sup>a</sup> TOF value is estimated from TON and reaction time.

the reaction rates, which implies the deactivation of the catalyst.

The third paper by Kumar *et al.*<sup>22</sup> reports the results for the conversion of glycerol to LA using four NNN pincer-Ru catalysts. When 0.58 equivalent base per mole of glycerol is used, these catalysts show low activities for glycerol conversion. However, when 1 equivalent base per mole of glycerol is used, a significant increase in catalytic activity is observed for [[<sup>Bim</sup>2NNNRuCl(PPh<sub>3</sub>)<sub>2</sub>]Cl] (Table 1).<sup>22</sup> Two ruthenium complexes with the PF<sub>6</sub><sup>-</sup> and Cl<sup>-</sup> anions, [[<sup>Bim</sup>2NNNRuCl(PPh<sub>3</sub>)<sub>2</sub>]PF<sub>6</sub>] and [[<sup>Bim</sup>2NNNRuCl(PPh<sub>3</sub>)<sub>2</sub>]Cl] show similar catalytic activity.<sup>22</sup> The complexes (<sup>Bu</sup>2NNNRuCl<sub>2</sub>(PPh<sub>3</sub>) and (<sup>Ph</sup>2NNNRuCl<sub>2</sub>(PPh<sub>3</sub>) provide lower catalytic activity than that of [[<sup>Bim</sup>2NNNRuCl(PPh<sub>3</sub>)<sub>2</sub>]Cl] without a significant change in selectivity for LA.<sup>22</sup> The highest activities were observed using ethanol as a solvent among the other solvents.<sup>22</sup> All reactions had to be carried out under an argon atmosphere because of the air sensitivity of the complexes.<sup>22</sup>

A 2018 paper<sup>23</sup> reported the synthesis of a series of iridium and ruthenium complexes with alkyl- and arylsulfonate-functionalized N-heterocyclic carbene (NHC) ligands and their employment as homogeneous catalysts in the conversion of glycerol to LA. The presence of the sulfonate group on the NHC ligand was reported to enhance the solubility of the complexes in polar protic solvents with minimal influence on the electron-donating ability of the NHC ligand. Thus, the sulfonate functionalization of NHC ligands renders the complexes very soluble in water, resulting in significant improvement in catalytic activity for the glycerol to LA conversion as compared to non-sulfonated analogues.<sup>23</sup> Among the catalysts tested for the glycerol conversion, the water-soluble Na[(NHC-ph-SO<sub>3</sub>)<sub>2</sub>-Ir(CO)<sub>2</sub>] complex provides the highest activity under microwave heating at 140 °C in the presence of 1 equivalent of KOH per mole of glycerol (Table 1).<sup>23</sup> The catalysts have been shown to have similar activity and selectivity for LA, starting with crude or pure glycerol.<sup>23</sup>

The conversion of glycerol to LA was also performed in a fed-batch reactor starting with glycerol and sodium hydroxide, that is, without catalyst.<sup>24,25</sup> A conversion of 93% of glycerol and selectivity of 82% for LA were achieved in the fed-batch process with 1.1 M initial glycerol concentration, 0.2 M NaOH concentration for 220 min at 300 °C. The corrosiveness toward the stainless steel reactor in glycerol conversion in the fed-batch process was also investigated by varying the NaOH concentration and measuring the concentration of Fe<sup>3+</sup> present in the

solution at the end of the reaction.<sup>24</sup> It was found that the concentration of Fe<sup>3+</sup> ions in the solution at the end of the reaction (thus the corrosiveness toward the reactor) decreased from 9.5 to 1.5 ppm when the initial concentration of NaOH was reduced from 1.25 M to 0.2 M. It is noteworthy that sodium hydroxide does not act as a catalyst for the conversion of glycerol to LA, in contrast to the claim of the paper.<sup>24</sup> The concentration of iron(III) ions was too low to have a measurable catalytic effect. Application of the fed-batch reactor for the conversion of crude glycerol gave 92.4% glycerol conversion and 72.9% selectivity for the LA. The decreases in conversion and selectivity were attributed to the high soap content of crude glycerol.<sup>24</sup>

### 3. Heterogeneous catalysts in the conversion of glycerol to LA

#### 3.1. Colloidal metal(0) nanoparticles

Using the colloidal metal nanoparticles is an auspicious way of increasing the catalytic performance due to the high fraction of surface atoms.<sup>26</sup> A recent paper by Wang *et al.*<sup>19</sup> reported the preparation of the PEG-stabilized bimetallic copper(0)-palladium(0) nanoparticles with various compositions as well as the monometallic copper(0) and palladium(0) nanoparticles, which have been tested as catalysts in the oxidation of glycerol in an aqueous solution of glycerol with a NaOH/glycerol molar ratio of 1.0 or 1.3, and a catalyst/glycerol mass ratio of 2 : 100 at 180–220 °C for 2.0 h. The bimetallic CuPd<sub>x</sub>/PEG nanoparticles have superior catalytic activity in glycerol oxidation as compared to the monometallic ones (Table 2). An increase in the palladium content of bimetallic nanoparticles resulted in the enhancement of the conversion of glycerol. The highest glycerol conversion (99.6%) was obtained using CuPd<sub>5</sub>/PEG catalyst.<sup>19</sup> However, the highest selectivity (95.3%) to LA was achieved by CuPd<sub>2</sub>/PEG catalyst.<sup>19</sup> Increasing the reaction temperature caused an increase in the glycerol conversion but a decrease in the selectivity for LA. A similar effect was also observed for increasing the reaction time: 100% conversion of glycerol was achieved upon extending the reaction time to four hours with the CuPd<sub>5</sub>/PEG catalyst but the selectivity for LA dropped to 92.8% for the reaction using the CuPd<sub>2</sub>/PEG.<sup>19</sup>

#### 3.2. Metal(0) nanoparticles supported on metal oxides

Copper(0),<sup>27,28</sup> platinum(0),<sup>29,30</sup> palladium(0),<sup>31</sup> nickel(0),<sup>33</sup> and trimetallic nanoparticles<sup>32</sup> supported on metal oxides have been



**Table 2** The parameters and results of the catalytic conversion of glycerol to LA in a basic medium by using colloidal metal nanoparticles and metal catalysts supported on metal oxides

Catalysts	Particle size (nm)		Surface area (m <sup>2</sup> g <sup>-1</sup> )	Metal loading (wt%)	TOF (h <sup>-1</sup> )	Time (h)	T (°C)	Select. (%)	Conver. (%)	Ref.
	Cu/Pd									
CuPd <sub>0.5</sub> /PEG	15.4/2.7	—	—	5	—	2	220	67.2	96.4	19
CuPd <sub>1</sub> /PEG	15.8/3.1	—	—	—	—	—	—	83.1	97.2	—
CuPd <sub>2</sub> /PEG	15.6/4.0	—	—	—	—	—	—	89.3	99.2	—
CuPd <sub>3</sub> /PEG	15.9/4.3	—	—	—	—	—	—	85.8	99.5	—
CuPd <sub>4</sub> /PEG	15.1/5.8	—	—	—	—	—	—	80.6	100	—
CuPd <sub>5</sub> /PEG	15.3/5.9	—	—	—	—	—	—	77.7	100	—
Cu(16)/MgO	—	—	—	—	150.7	2	230	85	82	27
Cu(16)/ZrO <sub>2</sub>	44.5	—	—	—	—	—	—	89	40	—
Cu(16)/HAP	33.8	—	—	—	116.3	—	—	84	85	—
Ni <sub>0.1</sub> /HAP	14	70.9	—	—	—	2	200	93.7	79.2	33
Ni <sub>0.2</sub> /HAP	16	65.4	—	—	—	—	—	94.7	92.1	—
Ni <sub>0.3</sub> /HAP	17	62.8	—	—	—	—	—	92.3	94.0	—
Ni <sub>0.4</sub> /HAP	17	60.4	—	—	—	—	—	89.8	96.0	—
Cu/Al <sub>2</sub> O <sub>3</sub>	31.8	323	—	15.8	—	3–6	240	92.5	88.6	28
Cu/ZnO	25.8	<20	—	16.2	—	—	—	89.0	84.2	—
Cu/MgO	12.0	48	—	15	—	—	—	90.0	95.4	—
Pt/ZnO	45.0	358	—	—	2632	30	240	60	97.0	29
Pt/MgO	21.2	<20	—	—	1297	—	—	55	93.6	—
Pt/Al <sub>2</sub> O <sub>3</sub>	2.4	<27	—	—	124	—	—	45	95.4	—
Pt/ZrO <sub>2</sub>	—	—	—	1.2	—	24	180	84	94	34
2Pt/ZrO <sub>2</sub> -550-R100	—	—	—	2.1	—	4.5	160	97	56	30
2Pt/ZrO <sub>2</sub> -550-R250	1.4	29	—	—	995	—	—	99	96	—
2Pt/ZrO <sub>2</sub> -550-R400	—	—	—	—	—	—	—	97	88	—
2Pt/ZrO <sub>2</sub> -DR250	—	—	—	—	—	—	—	97	71	—
Pd <sub>0.75</sub> /HAP	—	—	—	0.75	1091	1.5	230	82	85	31
Pd <sub>1.5</sub> /HAP	—	—	—	1.50	1143	—	—	90	89	—
Pd <sub>3</sub> /HAP	—	—	—	3.00	1274	—	—	95	99	—
Au/CeO <sub>2</sub>	—	131	—	0.7	—	8	220	92.6	75.5	35
AuCu/CeO <sub>2</sub>	6.3	114	—	0.8–1.0	—	—	—	91.2	77.8	—
1% Au/CeO <sub>2</sub>	—	—	—	0.95	—	—	90	83.0	98.0	42
3% Au/CeO <sub>2</sub>	<5	—	—	2.74	—	—	—	79.7	98.0	—
5% Au/CeO <sub>2</sub>	<5	—	—	4.59	—	—	—	79.0	98.0	—
Au/CeO <sub>2</sub>	—	—	—	1	365.7	—	90	67.5	a	43
Au/ZrO <sub>2</sub>	—	—	—	—	362.0	—	—	68.5	—	—
Au/Fe <sub>2</sub> O <sub>3</sub>	—	—	—	—	348.9	—	—	69.2	—	—
Au/Al <sub>2</sub> O <sub>3</sub>	—	—	—	—	334.1	—	—	70.8	—	—
Au/TiO <sub>2</sub>	—	—	—	—	374.4	—	—	73.8	—	—
Pt/TiO <sub>2</sub>	—	—	—	—	405.2	—	—	84.8	—	—
Pd/TiO <sub>2</sub>	—	—	—	—	9.1	—	—	10.3	—	—
AuPt/TiO <sub>2</sub> (1 : 1)	—	—	—	—	517.1	—	—	85.6	—	—
AuPt/TiO <sub>2</sub> (3 : 1)	—	—	—	—	507.4	—	—	84.3	—	—
AuPt/TiO <sub>2</sub> (1 : 3)	—	—	—	—	501.3	—	—	85.3	—	—
Au/TiO <sub>2</sub> + Pt/TiO <sub>2</sub> (1 : 1)	—	—	—	—	386.7	—	—	81.5	—	—
	—	—	—	—	389.8	—	—	79.3	—	—
Pd <sub>1</sub> Ni <sub>1</sub> O <sub>x</sub> /TiO <sub>2</sub>	3	—	—	2.5	—	2	90	51.6	44.0	49
Pt <sub>4</sub> Ni <sub>1</sub> O <sub>x</sub> /TiO <sub>2</sub>	—	—	—	—	—	—	—	62.1	45.9	—
Pt <sub>2</sub> Ni <sub>1</sub> O <sub>x</sub> /TiO <sub>2</sub>	—	—	—	—	—	—	—	63.8	49.2	—
Pt <sub>1</sub> Ni <sub>1</sub> O <sub>x</sub> /TiO <sub>2</sub>	—	—	—	—	—	—	—	73.7	58.0	—
Pt <sub>1</sub> Ni <sub>2</sub> O <sub>x</sub> /TiO <sub>2</sub>	—	—	—	—	—	—	—	62.3	47.1	—
Pt <sub>1</sub> Ni <sub>4</sub> O <sub>x</sub> /TiO <sub>2</sub>	—	—	—	—	—	—	—	57.7	33.0	—
Au/nCeO <sub>2</sub>	—	—	—	0.4	1040	0.5	100	60	76	50
Pt/nCeO <sub>2</sub>	—	—	—	0.5	1120	—	—	68	82	—
AuPt/nCeO <sub>2</sub>	—	—	—	0.4(Au), 0.3(Pt)	1350	—	—	80	99	—
Au/nCeO <sub>2</sub> + Pt/nCeO <sub>2</sub>	—	—	—	—	1220	—	—	65	90	—
Ru–Zn–Cu(i)/HAP	1.6	—	—	7.49(Ru) 9.78(Zn) 0.49(Cu)	—	21	140	82.7	100	32
Au/LLaO	4.1	—	—	—	—	14	90	64.4	60.7	53
Au/LPrO	3.3	32.8	—	—	—	—	—	66.8	68.2	—
Au/LSmO	4.9	—	—	—	—	—	—	60.2	53.7	—
Au/LGdO	5.4	—	—	—	—	—	—	55.4	52.4	—
Au/LDyO	5.0	—	—	—	—	—	—	65.1	51.4	—





tested as heterogeneous catalysts for the conversion of glycerol to LA in a basic medium. The results of catalytic investigations reported in those papers are listed in Table 2 along with the optimized parameters for glycerol oxidation to LA catalysed by the metal(0) nanoparticles supported on metal oxides.

### 3.2.1. Copper(0) nanoparticles supported on metal oxides.

The first paper by Wang *et al.*<sup>27</sup> reported the use of copper(0) nanoparticles supported on the surface of magnesium oxide (MgO), zirconia (ZrO<sub>2</sub>), or hydroxyapatite (HAP) as catalysts for the conversion of glycerol to LA in alkaline medium. Copper(0) nanoparticles were obtained from the reduction of copper(II) ions impregnated on the surface of supporting materials. The obtained nanocatalysts were denoted by the mass ratio of copper *X* to 100 support as Cu(*X*)/MgO, Cu(*X*)/ZrO<sub>2</sub>, and Cu(*X*)/HAP. Since the copper to support ratio of *X*:100 was used instead of percentage to give the composition of materials, the catalyst presumably contains major impurities in addition to copper and support.<sup>27</sup> The catalytic activity of the supported copper(0) nanoparticles with various Cu loadings was tested for the conversion of glycerol to LA in a 100 mL aqueous solution containing 1.0 M glycerol, 1.1 M NaOH, and 0.46 g catalyst at 230 °C for 2–8 h. First of all, both the glycerol conversion and selectivity for LA were found to increase with the increasing Cu loading for all the supported copper(0) catalysts. However, the nanocatalysts showed different variations in the activity and selectivity with time, depending on the support and Cu loading. For all the catalysts in that paper,<sup>27</sup> prolonging the reaction time caused the glycerol conversion to increase. The highest conversion (99%) was obtained using Cu(16)/MgO at the end of 8 h. Another noteworthy observation is that for the highest loading of Cu(16)/MgO and Cu(16)/HAP nanocatalysts, the glycerol conversion increased while the LA selectivity decreased with time.<sup>27</sup> For the highest loading of Cu(16)/ZrO<sub>2</sub> nanocatalyst, both the glycerol conversion and LA selectivity increased as the reaction proceeded.<sup>27</sup> The highest catalytic activity and selectivity for the conversion of glycerol to LA are listed in Table 2 for the Cu(*X*)/MgO, Cu(*X*)/ZrO<sub>2</sub>, and Cu(*X*)/HAP nanocatalysts.

The reusability of the nanocatalysts was also tested in the case of the Cu(16)/HAP nanocatalyst for the conversion of glycerol to LA.<sup>27</sup> In the reusability test, the catalyst was separated from the solution by centrifugation after the completion of the reaction and used for the next run under the same conditions. After four runs of the reusability test for the Cu(16)/HAP catalyst, the glycerol conversion decreased from 91% to 86%, while the LA selectivity decreased from 90% to 88%. The slight decrease in catalytic activity and selectivity may be attributed to the loss of materials during the separation and redispersion processes as the leaching test showed a negligible decrease in the ratio of copper to HAP from 15.86 : 100 to 15.84 : 100.<sup>27</sup>

The higher catalytic activities of the Cu/HAP and Cu/MgO nanocatalysts were attributed to the higher basicity of the HAP and MgO supports as compared to that of ZrO<sub>2</sub>. The lower catalytic activity of the Cu/ZrO<sub>2</sub> nanocatalyst was reported to be due to the small surface area of the zirconia support. It is noteworthy that the TOF values of Cu/ZrO<sub>2</sub> nanocatalysts were not reported for the transformation of glycerol in that paper.<sup>27</sup> A

reason for not giving the catalytic activity may be the formation of polymeric side products in addition to LA in the presence of Cu/ZrO<sub>2</sub> nanocatalysts while less than 3% of side products such as OA, FA, AA, and PAL were obtained from the reaction of glycerol when Cu/MgO and Cu/HAP were used as catalysts.<sup>27</sup> Some insights were also given into the formation of LA and side-products from glycerol in the presence of copper(0) nanoparticles, which will be taken into account for the discussion of possible mechanisms of the glycerol transformation in a later section (*vide infra*).

Another paper in the same year by Manfro *et al.*<sup>28</sup> similarly reports the use of metal oxide-supported copper nanoparticles as catalysts for the glycerol conversion to LA in a continuous system using a fixed-bed reactor. CuO was first supported on the surface of three different oxides, Al<sub>2</sub>O<sub>3</sub>, ZnO, or MgO, with a CuO loading of 20 wt%. The prepared CuO samples were then *in situ* reduced by H<sub>2</sub> at 450 °C in the reactor, yielding the putative Cu/Al<sub>2</sub>O<sub>3</sub>, Cu/ZnO and, Cu/MgO catalysts. It is noteworthy that the reduction of copper(II) oxide to copper(0) was completed by 94.5% for Cu/Al<sub>2</sub>O<sub>3</sub>, 86.1% Cu/ZnO, and 70.7% for Cu/MgO. Nevertheless, the Cu/Al<sub>2</sub>O<sub>3</sub>, Cu/ZnO and Cu/MgO nanoparticles were employed as catalysts in the continuous production of LA from glycerol in alkaline solution at 240 °C and 36 atm and found to show the highest glycerol conversion and LA selectivity in the presence of 1 equivalent of NaOH per mole of glycerol.<sup>28</sup> All the three copper(0) nanocatalysts were found to exhibit similar high glycerol conversion and high LA selectivity (Table 2). The similarity in the glycerol conversion and LA selectivity was attributed to the compensation between the basicity and copper metal surface area of catalysts. It is noteworthy that among the three catalysts, Cu/MgO provides the highest conversion of glycerol (95.4%) under the same conditions. Another noteworthy observation is that only PDO was obtained in a low selectivity of less than 10% as a side product in addition to the trace amount of acetol (hydroxyacetone).

Stability tests were applied on all three nanocatalysts using NaOH/glycerol with a molar ratio of 1 over 30 h.<sup>28</sup> Glycerol conversion reached stability over 2 h for Cu/Al<sub>2</sub>O<sub>3</sub> and Cu/MgO, while a period of 5 h was required for Cu/ZnO. The longer time requirement of Cu/ZnO for the stabilization of glycerol conversion was attributed to the oxidation of copper(0) to form Cu<sub>2</sub>O. Cu/ZnO and Cu/MgO displayed higher LA selectivity of around 90–95%, but the LA selectivity was approximately 82% for Cu/Al<sub>2</sub>O<sub>3</sub> after the initial period.<sup>28</sup> As such, the stability tests of the catalysts demonstrated that Cu/ZnO and Cu/MgO catalysts have high reusability, while a small catalytic deactivation was observed for Cu/Al<sub>2</sub>O<sub>3</sub> over 30 h. The reaction pathways proposed in that paper<sup>28</sup> will be discussed in a later section.

**3.2.2. Nickel(0) nanoparticles supported on metal oxides.** Nanosized hydroxyapatite-supported nickel(0) nanoparticles (Ni<sub>x</sub>/HAP) were found to effectively catalyse the conversion of high-concentrated glycerol (1.5–3 M) to LA in the presence of NaOH in an aqueous solution.<sup>33</sup> The catalytic activities of the Ni<sub>x</sub>/HAP nanocatalysts are always higher than that of the sole metallic nickel(0) nanoparticles for the conversion of glycerol to LA. When the reaction is started with Ni<sub>0.2</sub>/HAP catalyst with the



initial NaOH to glycerol molar ratio of 1.1 at 200 °C one obtains a glycerol conversion of 92.1% and LA selectivity of 94.7%.<sup>33</sup> The Ni<sub>0.3</sub>/HAP and Ni<sub>0.4</sub>/HAP nanocatalysts show higher glycerol conversion of 94% and 96%, respectively, but lower selectivity for LA of 92.3% and 89.8%, respectively, under the same conditions (Table 2). Increasing the reaction temperature to 240 °C has a positive influence on the glycerol conversion but has a reverse effect on LA selectivity for all the nanocatalysts with various compositions. Glycerol conversion increased to 97.0% while LA selectivity dropped to 81% for the Ni<sub>0.2</sub>/HAP catalyst at 240 °C. The higher selectivity for LA but lower glycerol conversion were obtained when the reaction was carried out for 1 h at 200 °C. The highest selectivity of 96.4% was achieved by the Ni<sub>0.2</sub>/HAP catalyst in 1 h reaction at 200 °C.<sup>33</sup>

**3.2.3. Platinum(0) nanoparticles supported on metal oxides.** The research group of Manfro<sup>29</sup> also investigated the LA production from glycerol in an alkaline medium by employing platinum(0) nanoparticles supported on Al<sub>2</sub>O<sub>3</sub>, ZnO, and MgO in a continuous flow reactor system over a period of 30 h. Platinum(IV) oxide was first supported on the surfaces of three oxides Al<sub>2</sub>O<sub>3</sub>, ZnO or MgO with a metal loading of 0.5 wt% PtO<sub>2</sub>. Then, the prepared platinum(IV) oxide samples were *in situ* reduced by H<sub>2</sub> at 450 °C in the reactor yielding the Pt/Al<sub>2</sub>O<sub>3</sub>, Pt/ZnO, and Pt/MgO catalysts. The three catalysts showed a catalytic activity order of Pt/ZnO > Pt/MgO > Pt/Al<sub>2</sub>O<sub>3</sub> (Table 2) for the glycerol conversion when the reaction was performed starting with the space velocity (WHSV) of 2 h<sup>-1</sup>, 10 vol% glycerol solution and NaOH/glycerol molar ratio of 1.0 at 240 °C. Note that the basicity order of the supports used for platinum(0) nanoparticles was MgO > ZnO > Al<sub>2</sub>O<sub>3</sub>. The highest catalytic activity (TOF = 2632 h<sup>-1</sup>) and LA selectivity (80%) were obtained by Pt/ZnO nanoparticles at 240 °C. The variations in the glycerol conversion as well as in the LA and PDO selectivity with temperature have been investigated using the Pt/ZnO nanocatalysts and the results are redisplayed in Fig. 1. The most favourable temperature for the glycerol conversion and LA selectivity appears to be in the range of 200–240 °C for the Pt/ZnO nanocatalyst. All three catalysts have allegedly high stability during the glycerol conversion for the period of up to 30 h. The stability order of the catalysts follows Pt/ZnO > Pt/MgO > Pt/Al<sub>2</sub>O<sub>3</sub>.

A 2015 paper<sup>34</sup> reported the use of zirconia-supported platinum(0) nanoparticles to catalyse glycerol oxidation starting with neat glycerol of 85% purity at 180 °C and 30 bar pressure of helium as an inert gas. Compared to the Pt/TiO<sub>2</sub> and Pt/C catalysts, Pt/ZrO<sub>2</sub> nanoparticles showed much higher glycerol conversion (95%) and LA selectivity (84%) in the 24 h reaction (Table 2).

Zirconia-supported platinum(0) nanoparticles were prepared by atomic trapping and were used as catalysts for the one-pot transfer hydrogenation between glycerol and cyclohexene to produce LA and cyclohexane.<sup>30</sup> The catalysts were denoted as aPt/ZrO<sub>2</sub>-b-Rc, where *a* is the wt% Pt loading, *b* is the calcination temperature, and *c* is the reduction temperature.<sup>30</sup> Changing the calcination or reduction temperature resulted in decreasing both glycerol conversion and LA selectivity while keeping the platinum loading at 2 wt% Pt and the reaction conditions were

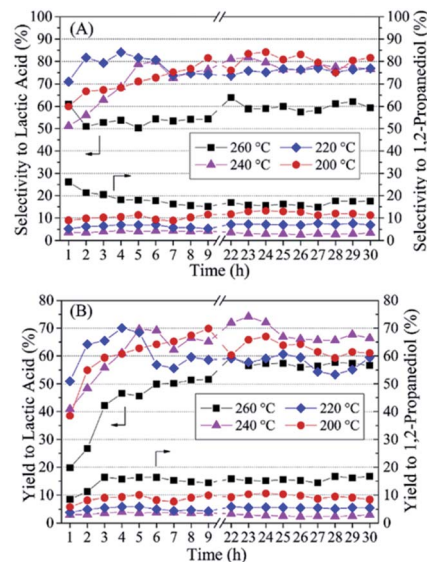


Fig. 1 (Reproduction of Fig. 5 from ref. 29). Lactic acid (LA) and 1,2-propanediol (1,2-PDO) selectivity (A) and yield (B) at different temperatures/pressures (200 °C/20 atm; 220 °C/25 atm; 240 °C/35 atm; 260 °C/46 atm) using Pt/ZnO catalyst. Reaction conditions: NaOH/glycerol  $\frac{1}{4}$ , WHSV  $\frac{1}{2}$  h<sup>-1</sup> and 10 vol% glycerol solution. Reproduced with permission.<sup>29</sup> Copyright 2016 Elsevier Inc.

the same. The 2Pt/ZrO<sub>2</sub>-550-R250 catalyst prepared without calcination showed 97% LA selectivity but a glycerol conversion value of 71%. The 2Pt/ZrO<sub>2</sub>-550-R250 catalyst showed the highest selectivity for LA (99%) with a glycerol conversion of 96% at 160 °C for 4.5 h under a nitrogen atmosphere with a pressure of 20 bar. The catalytic activity of only 2Pt/ZrO<sub>2</sub>-550-R250 was reported to be TOF = 995 h<sup>-1</sup>. Note that this is the highest activity reported for the selective conversion of glycerol to LA at such a low temperature of 160 °C. The reusability of the highest activity 2Pt/ZrO<sub>2</sub>-550-R250 catalyst was tested for five consecutive cycles under putatively identical conditions. A dramatic decrease in glycerol conversion associated with an increase in the size of Pt nanoparticles upon aggregation was observed from 96% to 54% while the catalyst preserved the LA selectivity.<sup>30</sup>

**3.2.4. Palladium(0) nanoparticles supported on metal oxides.** Another paper by Wang *et al.*<sup>31</sup> reported the preparation of palladium(0) nanoparticles supported on hydroxyapatite with three different loadings of 0.75%, 1.5%, and 3 wt% Pd, denoted as Pd<sub>0.75</sub>/HAP, Pd<sub>1.5</sub>/HAP, and Pd<sub>3</sub>/HAP, respectively. These were tested as catalysts for the conversion of glycerol to LA in the presence of 1.1 equivalent NaOH per mole of glycerol and 230 °C as optimized in a previous study of the same research group.<sup>27</sup> The obtained results are also listed in Table 2. The highest glycerol conversion of 99% and LA selectivity of 95% were obtained by using Pd<sub>3</sub>/HAP over 90 min at 230 °C, which provided the highest catalytic activity of TOF = 1274 h<sup>-1</sup> for the oxidation of glycerol to LA.<sup>31</sup> The reusability of Pd<sub>3</sub>/HAP was also tested in the conversion of glycerol to LA by separating the catalyst from the solution by centrifugation after the completion of the reaction, and it was used for the next reaction run under the



same conditions. After the five runs of the reusability test for the Pd<sub>3</sub>/HAP catalyst, the glycerol conversion decreased from 99% to 93% and the LA selectivity decreased from 95% to 94%. Accordingly, the TOF value for the glycerol conversion in the five consecutive runs decreased in the order of 1274, 1271, 1245, 1220, and 1194 h<sup>-1</sup>, respectively. The slight decrease in the catalytic activity and selectivity of the Pd<sub>3</sub>/HAP catalyst is ascribed to the leaching of the Pd from the support surface to the solution as the initial amount of 3.0 wt% Pd was determined to be 2.8% after five runs of catalytic conversion of glycerol to LA in the reusability tests.<sup>31</sup>

**3.2.5. Multimetallic nanoparticles supported on metal oxide.** A 2019 paper by Hernandez *et al.*<sup>35</sup> reported the use of monometallic gold and bimetallic gold–copper nanoparticles supported on ceria (Au/CeO<sub>2</sub> and AuCu/CeO<sub>2</sub>, respectively) as catalysts for the selective conversion of glycerol to LA in an alkaline medium. Although a hydrogen reduction was reported to have been performed after calcination at 400 °C for obtaining Au/CeO<sub>2</sub> and AuCu/CeO<sub>2</sub> nanoparticles, no compelling evidence has been provided for the existence of metallic copper(0). Nevertheless, the putative Au/CeO<sub>2</sub> and AuCu/CeO<sub>2</sub> nanoparticles were found to provide high glycerol conversion and LA selectivity in the presence of 1 equivalent of NaOH per mole of glycerol at 220 °C (Table 2). The higher glycerol conversion obtained by bimetallic as compared to monometallic nanocatalyst is to be noted even though both provide similar LA selectivity. Although as a reducible oxide support ceria has been shown to provide high catalytic activity for the supported transition metal(0) nanoparticles in many reactions generating H<sub>2</sub> gas,<sup>36–41</sup> the catalytic activity of AuCu/CeO<sub>2</sub> and Au/CeO<sub>2</sub> nanoparticles in the conversion of glycerol to LA seems to be low.<sup>35,42</sup> The glycerol conversion and LA selectivity obtained by Au/CeO<sub>2</sub> nanoparticles with different metal loadings are also given in Table 2.<sup>42</sup>

A 2010 paper<sup>43</sup> reported the activity and selectivity of titania supported bimetallic gold(0)–platinum(0) nanoparticles with various Au/Pt atomic ratios for the aerobic glycerol oxidation at 90 °C atmospheric O<sub>2</sub> pressure in the presence of NaOH at similar glycerol conversions of *ca.* 30% and, for comparison, monometallic Au, Pt, and Pd nanoparticles and other supporting oxides such as CeO<sub>2</sub>, ZrO<sub>2</sub>, Al<sub>2</sub>O<sub>3</sub>, Fe<sub>2</sub>O<sub>3</sub>. The choice of TiO<sub>2</sub> support was based on the observation of high catalytic activity and LA selectivity in glycerol oxidation at atmospheric O<sub>2</sub> pressure as compared to the other supports (Table 2). The titania-supported bimetallic AuPt/TiO<sub>2</sub> nanoparticles with various Au/Pt atomic ratios (1 : 1, 3 : 1, 1 : 3) provide superior catalytic activity and LA selectivity in glycerol oxidation at *ca.* 30% conversion of glycerol, as well as lower selectivity for GLYA compared to the titania-supported monometallic Au, Pt, and Pd nanoparticles of similar particle sizes (Table 2). Notably, the bimetallic AuPt/TiO<sub>2</sub> catalysts retained the high LA selectivity of *ca.* 86% even at 100% glycerol conversion (Fig. 2), corresponding to approximately 86% yield of LA.<sup>43</sup>

An important insight into the mechanism of catalytic glycerol oxidation was obtained from the examination of the physical mixture of Au/TiO<sub>2</sub> and Pt/TiO<sub>2</sub> with Au/Pt = 1 : 1 in glycerol oxidation.<sup>43</sup> The catalytic activity and LA selectivity of this

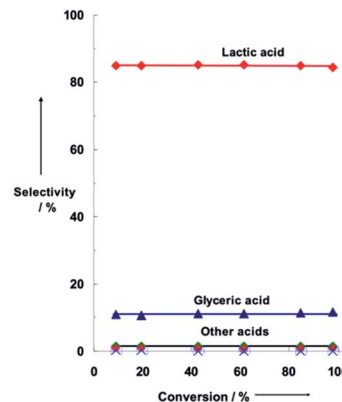


Fig. 2 (Reproduction of Fig. S5 from ref. 43). Selectivities of glycerol oxidation as a function of glycerol conversion at 90 °C on AuPt/TiO<sub>2</sub> with Au/Pt = 1/1, 1 atm O<sub>2</sub>, 2.5 × 10<sup>-5</sup> mmol metal, 0.22 M glycerol in water, molar ratio of NaOH/glycerol = 4 : 1. Reproduced with permission.<sup>43</sup> Copyright 2010 Wiley-VCH Verlag GmbH & Co.

physical mixture are essentially equal to the average of the activities and of the selectivities of the two individual components tested separately (Table 2). Therefore, the improved performance of the bimetallic AuPt/TiO<sub>2</sub> catalysts, compared to the monometallic Au/TiO<sub>2</sub> and Pt/TiO<sub>2</sub> catalysts, is not due to the coexistence of gold and platinum in the catalyst mixtures. Rather, it must be related somehow to the interaction between two metals in the bimetallic AuPt/TiO<sub>2</sub> catalysts. Such an interaction between two metals of bimetallic nanoparticles sitting on the surface of the oxide support can be suggested based on the previously reported IR results for CO adsorption on the AuPt/SiO<sub>2</sub> nanoparticles,<sup>44,45</sup> which suggests that strong ligands are capable of drawing platinum and that the strong bonds between surface oxides and platinum effectively concentrate Pt at the particle–support interface. This internal migration leads to the effective anchoring of the bimetallic nanoparticles to the oxide support, reducing their mobility and slowing down the particle agglomeration processes. The stabilization of small gold nanoparticles appears to be critically important for their catalytic activity when supported on oxides. The high catalytic activity is likely due to catalysis by gold but bimetallic sites may also play an important role. The interaction causes electron transfer from gold to platinum on the surface of Au–Pt/TiO<sub>2</sub> and then from platinum to oxide support, as shown by XPS analysis.<sup>46–48</sup>

Titania-supported nickel oxide-promoted platinum(0) and palladium(0) nanocatalysts have been tested for glycerol oxidation to LA in the presence of NaOH by Liu *et al.*<sup>49</sup> The molar ratio of Pt/Ni is denoted as *m* : *n* subscripts (Pt<sub>*m*</sub>Ni<sub>*n*</sub>O<sub>*x*</sub>/TiO<sub>2</sub>). The oxidation was carried out with O<sub>2</sub> flowing in the presence of NaOH/glycerol (4 : 1) at 90 °C using Pt<sub>*m*</sub>Ni<sub>*n*</sub>O<sub>*x*</sub>/TiO<sub>2</sub> and Pd<sub>1</sub>Ni<sub>1</sub>O<sub>*x*</sub>/TiO<sub>2</sub>. The presence of NiO<sub>*x*</sub> was observed to significantly increase glycerol conversion and LA selectivity as compared to Pt/TiO<sub>2</sub> and Pd/TiO<sub>2</sub> by presumably activating O<sub>2</sub> to atomic O for oxidation. The effects of catalyst compositions are listed in Table 2. The palladium(0) nanocatalyst (Pd<sub>1</sub>Ni<sub>1</sub>O<sub>*x*</sub>/TiO<sub>2</sub>) was only tested with a 1 : 1 molar ratio of Pd/Ni at 90 °C for





2 h. A glycerol conversion of 44% and LA selectivity of 51.6% were obtained by Pd<sub>1</sub>Ni<sub>1</sub>O<sub>x</sub>/TiO<sub>2</sub>, along with a high selectivity of 23.2% for GA. However, Pt<sub>1</sub>Ni<sub>1</sub>O<sub>x</sub>/TiO<sub>2</sub> with the same molar ratio exhibited the highest glycerol conversion (99.1%) and selectivity of LA (62.6%) for 4 h at the same temperature. Further increasing the Ni content was estimated to disable the contact between platinum(0) and the glycerol by the layer on the platinum(0) core. Pt<sub>1</sub>Ni<sub>1</sub>O<sub>x</sub>/TiO<sub>2</sub> was tested for five catalytic cycles, and no change in the molar ratio of Pt/Ni was observed. Glycerol conversion dropped to 57.2% from 99.1% with an increase in LA selectivity (72.9%) under the same conditions, where Pt<sub>1</sub>Ni<sub>1</sub>O<sub>x</sub>/TiO<sub>2</sub> showed the highest conversion and selectivity values. The coexistence of Pt and Ni enabled higher glycerol conversion with lower LA selectivity in comparison with Au–Pt/TiO<sub>2</sub>.<sup>43,49</sup>

A 2014 paper<sup>50</sup> reported the conversion of glycerol to LA in an alkaline medium with atmospheric O<sub>2</sub> using the monometallic gold and platinum as well as bimetallic gold-platinum nanoparticles supported on nanocrystalline ceria. The bimetallic AuPt/nCeO<sub>2</sub> catalyst showed better catalytic performance as compared to the monometallic ones in glycerol oxidation performed starting with 0.17 M glycerol, NaOH/glycerol molar ratio of 4, glycerol/metal ratio 680 at 100 °C and 5 bar O<sub>2</sub> (Table 2). Notably, the catalytic activity of a physical mixture of monometallic Au/nCeO<sub>2</sub> plus Pt/nCeO<sub>2</sub> nanocatalysts for glycerol conversion and LA selectivity is essentially equal to the average of the activities of the two individual components tested separately (Table 2). Therefore, the slightly improved catalytic performance of the bimetallic AuPt/nCeO<sub>2</sub> catalyst, compared to the monometallic Au/nCeO<sub>2</sub> and Pt/nCeO<sub>2</sub> catalysts, cannot be attributed to the coexistence of gold and platinum in the catalyst mixtures. Rather, it is due to the strong interaction between two metals and the oxide support in the bimetallic AuPt/nCeO<sub>2</sub> catalyst, which was supported by the XPS analysis.<sup>50</sup> The bimetallic AuPt/nCeO<sub>2</sub> catalyst is reported to have high reusability since it retained its activity in five successive runs of glycerol oxidation.<sup>50</sup>

The last paper by Han *et al.*<sup>32</sup> reported the employment of a HAP-supported trimetallic Ru–Zn–Cu(i)/HAP nanocatalyst for the conversion of glycerol to LA. However, there is a problem in using ruthenium-based catalysts in the production of LA from glycerol as ruthenium enables the cleavage of C–C bonds in hydrocarbons. Consequently, when the glycerol conversion to LA is catalysed by ruthenium nanoparticles in the presence of a base, the degradation of LA to FA inevitably occurs with the formation of methane and carbon dioxide.<sup>51</sup> The LA selectivity was shown to be significantly enhanced with the addition of copper(i) ions, which diminished the C–C bond cleavage.<sup>52</sup> The presence of Zn<sup>2+</sup> ion increased the 1,2-hydride shift of PAL in the intermediate step. As such, an improved selectivity (82.7%) for LA was achieved by using the Ru–Zn–Cu(i)/HAP nanocatalyst as compared to that obtained by Ru/HAP nanoparticles (selectivity, 63.7%) or by Ru–Zn/HAP nanoparticles (selectivity, 70.9%). Complete conversion of glycerol was achieved by using the Ru–Zn–Cu(i)/HAP nanoparticles after 21 h in the presence of 1 equivalent of NaOH per mole of glycerol.<sup>32</sup> The inspection of TEM images in Fig. 2 of that paper<sup>32</sup> revealed the uniform

dispersion of ruthenium(0) nanoparticles of less than 2 nm on the surface of HAP in the Ru–Zn–Cu(i)/HAP sample. The presence of copper(i) ions in the Ru–Zn–Cu(i)/HAP sample could effectively inhibit the cleavage of C–C bonds, leading to a significant improvement in the yield of LA. Thus, using the Ru–Zn–Cu(i)/HAP as a catalyst in the production of LA from glycerol provided the complete conversion of glycerol and 82.7% LA selectivity over 12 h in the presence of 1.5 equivalents of NaOH per mole of glycerol at 140 °C. It is noteworthy that this is the highest activity obtained at the lowest temperature ever reported for the catalytic conversion of glycerol to LA. The Ru–Zn–Cu(i)/HAP nanocatalyst was also shown to be highly reusable, retaining its initial catalytic activity for glycerol conversion and LA selectivity even in the fourth run of the reaction (Fig. 5 in that paper).<sup>32</sup>

Layered rare-earth hydroxide (LREH, RE = Y, La, Pr, Nd, Sm, Eu, Gd, Tb, Dy, Ho, Er, and Tm) nanosheets were used as supports for the gold(0) nanoparticles.<sup>53</sup> The LREH nanosheets supported gold(0) nanoparticles were prepared by the deposition–precipitation of HAuCl<sub>4</sub> and calcination and denoted as Au/LREO. The highest glycerol conversion (68.2%) with the highest LA selectivity (66.8%) was obtained using Au/LPrO among Au/LREO catalysts at 90 °C for 14 h under aerobic conditions. That was followed by glycerol conversion of 60.7% and LA selectivity of 64.4% over Au/LLaO. However, GA selectivity was also over 20% for those catalysts. Au/LSmO, Au/LGdO, and Au/LDyO showed around 50% glycerol conversion. For the rest of the catalysts, Au/LNdO, Au/LEuO, Au/LTbO, Au/LHoO, Au/LErO, and Au/LTmO, glycerol conversions were lower than 50%. The order of particle sizes of the catalysts was consistent with the decrease in glycerol conversion. Au/LPrO had the smallest gold(0) particle size of around 3.3 nm. The Au/LPrO catalyst exhibited lower glycerol conversion with LA selectivity as compared to the metal oxide-supported gold(0) nanoparticles Au/CeO<sub>2</sub> tested by Palacio *et al.*<sup>35</sup> for glycerol conversion to LA over 8 h at 220 °C. In comparison with Au/CeO<sub>2</sub> (ref. 50) tested at 90 °C, Au/LPrO showed much higher glycerol conversion and similar LA selectivity.

### 3.3. Metal/metal oxide nanoparticles

Herein, we review the papers on the glycerol oxidation performed starting with metal oxide nanoparticles that might be reduced under the reducing conditions of the reaction. The first paper by Shen *et al.*<sup>54</sup> reported the use of poly(vinylpyrrolidone)-stabilized copper(i) oxide nanoparticles (Cu<sub>2</sub>O/PVP) of different average particle sizes in the range of 115–423 nm as a catalyst for the conversion of glycerol to LA in the presence of a base. The Cu<sub>2</sub>O nanoparticles with the smallest average particle size of 115 nm provided the highest glycerol conversion and LA selectivity in the presence of 1.0 equivalent of NaOH per mole of glycerol at 230 °C (Table 3).<sup>54</sup> Although the prepared materials were characterized as Cu<sub>2</sub>O, it is not known whether Cu<sub>2</sub>O would be the active catalyst. Cu<sub>2</sub>O can readily be reduced to metallic copper under the reducing conditions of glycerol oxidation in the presence of a strong base such as NaOH.





**Table 3** The parameters and results of the catalytic conversion of glycerol to LA in a basic medium by using metal nanoparticles and metal oxides supported on metal oxides

Catalysts	Particle size (nm)	Surface area (m <sup>2</sup> g <sup>-1</sup> )	TOF (h <sup>-1</sup> )	Time (h)	T (°C)	Select. (%)	Conver. (%)	Ref.
Cu <sub>2</sub> O NPs	115	—	—	2	230	89.1	92.5	54
Cu <sub>PEG</sub>	36.9	—	21.8	2	230	91.1	94.1	55
Cu <sub>tween</sub>	49.5	—	21.6	—	—	89.5	93.2	—
Cu <sub>CTAB</sub>	93.0	—	21.2	—	—	87.1	91.3	—
Cu/SiO <sub>2</sub>	—	—	—	6	240	79.7	75.2	56
CuO/Al <sub>2</sub> O <sub>3</sub>	—	—	—	—	—	78.6	97.8	—
Cu <sub>2</sub> O	—	—	—	—	—	78.1	93.6	—
5%CuO/ZrO <sub>2</sub>	—	63	—	6	160	82.9	12.5	57
10%CuO/ZrO <sub>2</sub>	—	61	—	—	—	77.4	18.4	—
15%CuO/ZrO <sub>2</sub>	—	64	—	—	—	86.5	33.3	—
20%CuO/ZrO <sub>2</sub>	—	60	—	—	—	82.1	43.4	—
30%CuO/ZrO <sub>2</sub>	—	56	—	—	—	85.0	67.5	—
30%CuO/ZrO <sub>2</sub> -IM	—	56	—	—	—	78.7	52.7	—
30%CuO/ZrO <sub>2</sub> -CP	—	179	—	—	—	59.8	26.1	—
45%CuO/ZrO <sub>2</sub>	—	47	—	—	—	77.9	68.3	—
60%CuO/ZrO <sub>2</sub> -IM	—	38	—	—	—	74.2	64.7	—
5.7CuO/CeO <sub>2</sub>	—	113	—	8	220	55.2	27.4	58
9.9CuO/CeO <sub>2</sub>	—	127	—	—	—	71.1	45.6	—
17.8CuO/CeO <sub>2</sub>	—	97	—	—	—	80.3	70.3	—
26.1CuO/CeO <sub>2</sub>	—	84	—	—	—	74.4	87.3	—
Co <sub>3</sub> O <sub>4</sub> /CeO <sub>2</sub> -DP	—	84	—	8	250	69	74.4	59
Co <sub>3</sub> O <sub>4</sub> /CeO <sub>2</sub> -I	—	46	—	8	250	79.8	85.7	—
CuMg	14.6(Cu)	36	8.0	23–30	240	63.9	81.9	60
CuCa	14.1(Cu)	<20	7.5	—	—	59.1	87.8	—
Cu5CaMg	14.4(Cu)	25	10.7	—	—	78.0	96.4	—
Cu10CaMg	14.8(Cu)	30	10.2	—	—	72.5	91.0	—
Cu15CaMg	12.9(Cu)	25	10.7	—	—	68.1	96.4	—
Cu-Zn-Al	—	85	—	4	135	78.7	71.5	63
Cu-Cr	—	29	—	—	—	94.3	17.5	—

Without knowledge of the active catalyst, all the mechanistic discussions might be considered to be speculative.

Different-sized copper(0) nanoparticles with organic modifiers have been reported to be used as catalysts for the oxidation of glycerol to LA with the initial concentrations of glycerol and NaOH of 1.0 and 1.1 M, respectively, at 230 °C.<sup>55</sup> The smallest size copper(0) nanoparticle was obtained *via* a wet chemical reduction method using PEG, which was denoted as Cu<sub>PEG</sub> and exhibited the highest catalytic activity (21.8 h<sup>-1</sup>). Cu<sub>tween</sub> and Cu<sub>CTAB</sub> were prepared by the same method with stabilizer tween-80 and hexadecyl trimethyl ammonium bromide (CTAB), and Cu<sub>blank</sub> was synthesized without stabilizer. The average particle size increased on passing from Cu<sub>tween</sub> to Cu<sub>blank</sub> with a concomitant decrease in the catalytic activity. The same trend was also observed for both glycerol conversion and LA selectivity, which was associated with more copper(0) active sites as the average particle size decreased. The optimized LA selectivity values were reached for all copper(0) nanoparticles for 4 h at 230 °C. However, glycerol conversion continued to increase with the prolonged reaction until 8 h. Almost complete conversion of glycerol was achieved, even with using the Cu<sub>blank</sub> catalyst with a reaction time of 8 h. Only the recyclability of Cu<sub>PEG</sub> was tested after the separation from the reaction medium by centrifugation for four cycles under the same reaction conditions listed in Table 3. A slight decrease in glycerol conversion and LA

selectivity was observed without numerical values for change in the selectivity.

A 2011 paper by Chaudhari's group<sup>56</sup> reported the use of three different copper-based catalysts Cu/SiO<sub>2</sub>, Cu<sub>2</sub>O, and CuO/Al<sub>2</sub>O<sub>3</sub> for glycerol conversion to LA in an alkaline medium. The Cu/SiO<sub>2</sub>, Cu<sub>2</sub>O, and CuO/Al<sub>2</sub>O<sub>3</sub> catalysts provided glycerol conversions of 75.2%, 97.8%, and 93.6%, respectively, in the experiments performed starting with 3 g glycerol, NaOH/glycerol molar ratio of 1.1, and 3.5 mmol Cu in 30 mL aqueous solution at 14 bar and 240 °C over 6 h, with similar LA selectivity (Table 3).<sup>56</sup> The issue of whether Cu<sub>2</sub>O or CuO would have been reduced under the reducing conditions of the reaction was not addressed in that paper.<sup>56</sup> If the reduction would not have occurred, it is not possible to have a rational comparison of three different catalysts on three different supports. The reusability was tested only for the Cu<sub>2</sub>O catalyst in the glycerol conversion at 200 °C with a molar NaOH/glycerol ratio of 1.1. As shown in Fig. 1 of that paper,<sup>56</sup> the catalyst retained its initial activity in the four successive runs of glycerol oxidation, indicating the high stability of the catalyst under reaction conditions.

Zirconia-supported copper(II) oxide catalysts with various compositions have been reported to be tested for the conversion of glycerol to LA in 1.4 M glycerol solution with a NaOH/glycerol molar ratio of 1 at 180 °C under an inert atmosphere.<sup>57</sup> The



CuO/ZrO<sub>2</sub> catalyst with 30% Cu loading exhibited the highest glycerol conversion (100%) and selectivity for LA (94.6%) in 8 h reaction.<sup>57</sup> In the reusability test, there were variations in glycerol conversion while the LA selectivity remained constant in successive runs of glycerol oxidation. Although the glycerol oxidation started with the CuO/ZrO<sub>2</sub> precatalyst, the active catalyst is not known. In other words, it has never been investigated whether copper(II) oxide would undergo any reduction under the reducing conditions of the glycerol oxidation reaction at high temperatures.

Ceria-supported copper(II) oxide catalysts were prepared with various Cu loadings, denoted as XCuO/CeO<sub>2</sub> (X: copper loading%), and used in the selective conversion of glycerol to LA with a NaOH/glycerol molar ratio of 1 : 1 at 220 °C by the research group of Hernandez.<sup>58</sup> Bare CeO<sub>2</sub> was found to catalyse the glycerol oxidation, with low conversion (27.5%) and quite high selectivity (74.7%) for LA, for 8 h. Using the XCuO/CeO<sub>2</sub> catalysts caused a significant improvement in the conversion of glycerol as shown in Fig. 5a of that paper.<sup>58</sup> For example, the use of 26.1CuO/CeO<sub>2</sub> catalyst can provide a glycerol conversion of 87.3% with a similar LA selectivity of 74.4%. The highest selectivity of 80.3% for LA was obtained by a 17.8CuO/CeO<sub>2</sub> catalyst with a lower glycerol conversion of 70.3%. A closer look at the plots in Fig. 5a of that paper<sup>58</sup> showed an induction period, particularly in the presence of XCuO/CeO<sub>2</sub> catalysts with high Cu loading (X = 26.1 and 17.8%). Such an observation may imply the formation of an active catalyst during the glycerol oxidation, *i.e.* the reduction of oxide to lower oxidation states of metals. Another noteworthy point is the observation of glycerol conversion of 32% and 15% present at the commencement of the reaction for the two XCuO/CeO<sub>2</sub> catalysts with X = 26.1 and 17.8%, respectively (Fig. 5a of that paper<sup>58</sup>). More interestingly, the amount of glycerol conversion present at the commencement of the reaction was observed to be dependent on the concentration of NaOH (Fig. 8a of that paper<sup>58</sup>): using the 26.1CuO/CeO<sub>2</sub> catalyst, the value was reduced from 34% to 17% when the NaOH/glycerol molar ratio was halved. Thanks to the high-quality kinetics data provided in that paper,<sup>58</sup> all these details are now evident and, of course, they need to be further investigated for understanding the mechanism of the selective catalytic conversion of glycerol to LA. Although the XCuO/CeO<sub>2</sub> composites have been well characterized, their behaviour under the reducing conditions of glycerol oxidation at high temperatures has not been investigated.<sup>58</sup> In other words, the active catalyst in glycerol oxidation starting with the XCuO/CeO<sub>2</sub> precatalyst remains unknown. Bulk Cu<sub>2</sub>O and CuO were also tested as catalysts for glycerol oxidation under similar conditions, including the same Cu/glycerol molar ratio. CuO was found to provide higher glycerol conversion (66.6%) than that obtained by Cu<sub>2</sub>O (34.9%). This almost 2-fold difference in the glycerol conversion may arise from the 2-fold higher concentration of CuO than that of Cu<sub>2</sub>O as the same Cu concentration has been used in both cases (Fig. 9 of that paper<sup>58</sup>). Therefore, the conclusion that the copper(II) species would be more active than the copper(I) species in converting the glycerol to LA is likely incorrect. Once again, it needs to be noted that the active catalyst is still unknown in the glycerol conversion started with

copper oxide-based catalysts. The CuO/CeO<sub>2</sub> composite was also tested for reusability in glycerol conversion and the results in Fig. 10 of that paper<sup>58</sup> show that the glycerol conversion slightly decreases in the second and third runs and then starts to increase in the fourth and fifth runs, while the LA selectivity remains unaltered throughout the reusability test.

Another article by the Hernandez research group<sup>59</sup> reported the use of ceria-supported cobalt(II,III) oxide nanoparticles as catalysts for the conversion of glycerol to LA in an aqueous basic solution with the NaOH/glycerol molar ratio of 1 at 250 °C and 60 bar of N<sub>2</sub>. The glycerol conversion was found to be dependent on the method used to prepare the Co<sub>3</sub>O<sub>4</sub>/CeO<sub>2</sub> nanoparticles, namely, deposition-precipitation (DP) or impregnation (I). Co<sub>3</sub>O<sub>4</sub>/CeO<sub>2</sub>-DP has a larger specific surface area than Co<sub>3</sub>O<sub>4</sub>/CeO<sub>2</sub>-I (Table 3). Both the Co<sub>3</sub>O<sub>4</sub>/CeO<sub>2</sub>-DP and Co<sub>3</sub>O<sub>4</sub>/CeO<sub>2</sub>-I nanoparticles have a smaller surface area as compared to the parent CeO<sub>2</sub> particles. Co<sub>3</sub>O<sub>4</sub>/CeO<sub>2</sub>-I nanoparticles provide higher glycerol conversion (85.7%) and higher LA selectivity (79.8%) than those obtained by Co<sub>3</sub>O<sub>4</sub>/CeO<sub>2</sub>-DP nanoparticles (74.4% glycerol conversion and 69% LA selectivity). The reusability test was performed only for Co<sub>3</sub>O<sub>4</sub>/CeO<sub>2</sub>-I nanoparticles, indicating that both glycerol conversion and LA selectivity decreased significantly in the third run of glycerol oxidation.<sup>59</sup>

A recent paper by the Manfro<sup>60</sup> research group reported the preparation of CaO, MgO, and CaO/MgO-supported CuO catalysts by impregnation and calcination. The various mixed oxide catalysts were denoted as CuMg, CuCa, Cu5CaMg, Cu10CaMg, and Cu15CaMg without O for oxygen. The numbers showed the percentage of CaO loading in the mixed oxides. All the mixed oxides were employed as catalysts for the conversion of glycerol to LA in a continuous flow reaction system with 10 vol% glycerol solution, NaOH/glycerol molar ratio of 1, feed flow of 0.041 mL min<sup>-1</sup> at 240 °C and 35 atm.<sup>60</sup> The results are listed in Table 3. The Cu5CaMg, Cu10CaMg, and Cu15CaMg catalysts were found to have higher catalytic activity as well as higher LA selectivity than that obtained by CuMg and CuCa catalysts (Table 3). Unfortunately, no effort has been made to find out what the active catalyst would be.

The rapid conversion of glycerol to LA (in fact, the lactate ion) could be successfully achieved without side reactions under alkaline hydrothermal conditions by using a continuous flow reaction system.<sup>61</sup> The rapid conversion and high reaction yield (reaction: 2 min; yield: 90%) resulted from the rapid temperature shift, which is advantageous for the inhibition of side reactions.

The direct transformation of bioderived glycerol to LA under the catalysis of bimetallic CuPd<sub>x</sub> nanoparticles as well as monometallic Cu and Pd was investigated under hydrothermal conditions.<sup>62</sup>

A 2017 paper by Li *et al.*<sup>63</sup> reported the employment of the commercial catalysts Cu-Zn-Al (with a specific composition of 63.5% CuO, 24.7% ZnO, 10.1% Al<sub>2</sub>O<sub>3</sub>, and 1.3% MgO) and Cu-Cr (with a specific composition of 64% Cr<sub>2</sub>CuO<sub>4</sub>, 24% CuO, 6% BaO, 4% graphite, 1%CrO<sub>3</sub> and 1% Cr<sub>2</sub>O<sub>3</sub>) after hydrogen reduction for the transformation of glycerol to LA in an aqueous basic solution with the NaOH/glycerol ratio of 1.5 at a temperature between 100–175 °C under an inert nitrogen atmosphere.



Glycerol oxidation occurs presumably on the copper surface as both catalysts have been pre-reduced by H<sub>2</sub> gas. The Cu–Zn–Al catalyst displayed much higher performance for the conversion of glycerol to LA, which was attributed to the higher surface area and higher copper content of the former than that of the latter (Table 3). The Cu–Zn–Al catalyst was also tested for reusability in glycerol oxidation at 175 °C, whereby the glycerol conversion decreased from 59.73% to 51.86% and the LA was selectively decreased from 78.79% to 77.98% on passing from the first to the third run of glycerol oxidation. The rate of glycerol disappearance was reported to be first-order with respect to the glycerol concentration, and the rate constant increased linearly with catalyst concentration. These observations suggest that glycerol dehydrogenation on the copper surface is the rate-limiting step.

### 3.4. Metal(0) nanoparticles supported on carbonaceous materials

A recent paper by Ma *et al.*<sup>64</sup> reported the preparation of graphitic-carbon-layer-encapsulated Ni–NiO<sub>x</sub> core/shell nanoparticles (Ni–NiO<sub>x</sub>@C) by controlled oxidation of the pristine Ni@C nanoparticles, which have been employed as catalysts for the conversion of glycerol to LA in alkaline medium. Note that the subscript *x* denotes the percentage of NiO in Ni–NiO<sub>x</sub>@C although it has been estimated from the surface analysis by XPS and has not been given for the respective samples in catalysis. In the sample designations, the number following the formula indicates the oxidation temperature (150, 175, 200, or 250 °C) of Ni@C nanoparticles. Fig. 3a shows the results of glycerol oxidation experiments performed starting with various Ni–NiO<sub>x</sub>@C catalysts in the presence of 1.1 equivalents of NaOH per mole of glycerol at 200 °C and 1.4 MPa for 30 min, while Fig. 3b shows the results of similar experiments with Ni–NiO<sub>x</sub>@C-200 at various temperatures. The inspection of Fig. 3 can convey the following points: (i) the catalytic activity and selectivity are in general low, (ii) the glycerol conversion doesn't correlate with the total amount of the products in all experiments, (iii) the highest yield for the LA obtained by the Ni–NiO<sub>x</sub>@C-200 catalyst at 200 °C is only 46.8% for 30 min. The low activity obtained in that study might be attributed to the allegedly encapsulated nanocatalysts by the graphitic carbon cover.<sup>64</sup> However, even such a conclusion needs to be considered with doubt as the materials characterization seems to be disputable in that paper.<sup>64</sup> Another noteworthy point is that it has not been addressed whether the Ni/NiO ratio would have been changed during the glycerol conversion under the reducing conditions of the reaction. Because of the magnetic nickel(0) core, the Ni–NiO<sub>x</sub>@C catalysts could be isolated using an external magnet and such an easy recovery of the catalyst could facilitate the reusability test. Indeed, the Ni–NiO<sub>x</sub>@C-200 catalyst was found to have high reusability as it retained its initial glycerol conversion and LA selectivity almost completely after five runs of glycerol oxidation.

A 2018 paper<sup>65</sup> reported the catalytic performance of graphite-supported nickel(0) nanoparticles in the conversion of glycerol to LA in NaOH aqueous solution. Graphite-supported

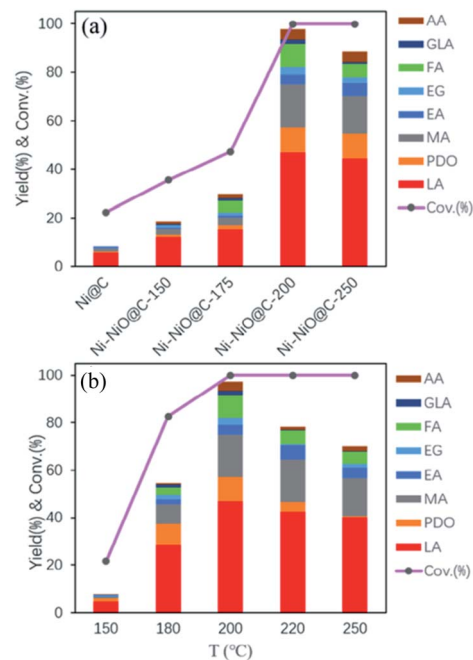


Fig. 3 (Reproduction of Fig. 6a and c, respectively, from ref. 64). (a) The results of glycerol oxidation experiments performed starting with various Ni–NiO<sub>x</sub>@C catalysts in the presence of 1.1 equivalent of NaOH per mole of glycerol at 200 °C and 1.4 MPa for 30 min. (b) The results of similar experiments as in (a) with the Ni–NiO<sub>x</sub>@C-200 catalyst at various temperatures. Reproduced with permission.<sup>64</sup> Copyright 2020 American Chemical Society.

nickel(0) nanoparticles with different Ni loadings were tested as catalysts in glycerol oxidation in an aqueous solution of 1.0 M glycerol and 1.1 M NaOH at 230 °C for 3 h. The Ni<sub>0.3</sub>/graphite nanoparticles (0.3 mmol nickel(0) per gram) with an average particle size of 33 nm provided the highest selectivity (92.1%) for LA (Table 4) while the Ni<sub>0.1</sub>/graphite nanoparticles with the smallest average particle size of 23 nm gave the highest TOF value of 59.4 h<sup>-1</sup> for the glycerol to LA conversion at 230 °C. The average particle size of nanoparticles had an expected adverse effect on the catalytic activity. Compared to the Ni–NiO<sub>x</sub>@C-200 catalyst,<sup>64</sup> the Ni<sub>0.3</sub>/graphite nanoparticles provided higher selectivity for LA with a similar glycerol conversion.<sup>65</sup> Although the glycerol conversion soared up to 99.3% with the use of Ni<sub>0.4</sub>/graphite nanoparticles, the selectivity for LA dropped down to 76.8%. Complete conversion of glycerol was achieved by Ni<sub>0.3</sub>/graphite at a reaction temperature of 250 °C but with a low LA selectivity of 80.4%. The reusability test was performed only for the Ni<sub>0.3</sub>/graphite nanocatalyst at 230 °C for 2 h. Although the nickel(0) nanoparticles were expected to be magnetic, the catalyst was recovered from the reaction solution by centrifugation for the reusability test. After four runs, the Ni<sub>0.3</sub>/graphite nanocatalyst essentially retained its initial activity and selectivity as shown in Fig. 6 of that paper.<sup>65</sup>

The catalytic activity of the activated carbon-supported platinum(0) (Pt/AC) nanoparticles for the oxidation of glycerol to LA in the presence of NaOH was reported in a 2016 paper by Zhan *et al.*<sup>66</sup> It was first shown that the experiment performed



**Table 4** The parameters and results of the catalytic conversion of glycerol to LA in a basic medium by using metal catalysts supported on carbonous oxides

Catalysts	Particle size (nm)	Surface area (m <sup>2</sup> g <sup>-1</sup> )	TOF (h <sup>-1</sup> )	Time (h)	T (°C)	Selectivity (%)	Conversion (%)	Ref.
Ni–NiO <sub>x</sub> /C-200	8.3	—	—	0.5	200	45.7	23.2	64
Ni–NiO <sub>x</sub> @C-200	8.2	—	—	—	—	46.8	100	—
Ni <sub>0.1</sub> /graphite	22.4	—	59.6	2	230	83.2	62.2	65
Ni <sub>0.2</sub> /graphite	29.5	—	39.2	—	—	88.9	77.4	—
Ni <sub>0.3</sub> /graphite	32.9	—	33.8	—	—	92.1	95.1	—
Ni <sub>0.4</sub> /graphite	35.1	—	26.5	—	—	76.8	99.3	—
Pt/AC	4.4	970.8	—	6	90	69.3	100	66
10% Pd/C	0.5–2.5	758	—	3	230	61.9	93.8	68
5% Pt/C	—	388	—	—	—	74.9	99.2	—
0.1%Cu–1.0%Pt/AC	—	991	257	4	90	66.9	43.7	69
0.2%Cu–1.0%Pt/AC	—	918	288	—	—	65.7	52.7	—
0.35%Cu–1.0%Pt/AC	—	—	—	—	—	72.9	68.2	—
0.5%Cu–1.0%Pt/AC	—	954	437	—	—	69.3	80.0	—
0.75%Cu–1.0%Pt/AC	—	—	—	—	—	67.5	62.7	—
1.0%Cu–1.0%Pt/AC	—	893	323	—	—	64.4	60.9	—
2.0%Cu–1.0%Pt/AC	—	905	236	—	—	49.0	42.8	—

without catalyst in the presence of 1 equivalent NaOH per mole of glycerol resulted in a glycerol conversion of 5.9% with a LA selectivity of 17.5% at 90 °C. Recall that a glycerol conversion of 93 mol% of glycerol and selectivity of 82 mol% for LA were achieved in the fed-batch process starting with 1.1 M initial glycerol concentration, 0.2 M NaOH concentration for 220 min at 300 °C.<sup>24</sup> Note that the experiment performed without a strong aqueous base in the absence or presence of catalyst yielded no LA from the oxidation of glycerol at all.<sup>24,66</sup> These results indicate that the presence of both the catalyst and the strong base is inevitable for the glycerol oxidation to LA at an appreciable rate. The glycerol conversion experiments were then performed starting with different strong bases of a base/glycerol molar ratio of 2 in the presence of Pt/AC catalyst with a Pt/glycerol molar ratio of 1/2400 at 90 °C. As seen from Table 2 of that paper,<sup>66</sup> the use of LiOH provided the highest LA selectivity of 60.1% with glycerol conversion as high as 60.4% under identical conditions. Inspection of the results in Table 4 of that paper<sup>66</sup> indicated that the Pt/AC catalyst provided the highest glycerol conversion of 100% and LA selectivity of 69.3% in the presence of LiOH/glycerol with a molar ratio of 1.5 and Pt/glycerol molar ratio of 1/2400 at 90 °C for 6 h. The reusability test of the Pt/AC nanocatalyst in the glycerol oxidation under the optimized conditions showed a decrease in the glycerol conversion from 63.6% to 52.9% after the five cycles (Fig. 4).<sup>66</sup> The decrease in glycerol conversion was attributed to the agglomeration of platinum(0) nanoparticles during the isolation and redispersion processes for the successive runs of oxidation.<sup>66</sup>

Detailed kinetic modelling of the Pt/C catalysed conversion of glycerol to LA, glycols, and alcohols with *in situ* formed hydrogen was reported.<sup>67</sup> Experimental concentration–time profiles were obtained in a batch slurry reactor at different glycerol concentrations, nitrogen partial pressures, and NaOH concentrations in a temperature range of 130–160 °C. At 130 °C, prolonging the reaction time facilitated the increase in the

formation of LA and PDO. However, the formation of alcohols (methanol, ethanol, and 2-propanol) increased rapidly at 145 and 160 °C. The effect of nitrogen pressure was also investigated on glycerol conversion and product selectivity. The increase in pressure from 0.3 to 3.5 MPa did not have a significant effect on the oxidation of glycerol to LA at 160 °C for 2 h.

A 2017 paper<sup>68</sup> also reported the employment of carbon-supported palladium(0) and platinum(0) nanocatalysts for the conversion of glycerol to LA in alkaline medium. The PdCl<sub>2</sub> and H<sub>2</sub>PtCl<sub>6</sub> precursors were impregnated on activated carbon, inappropriately designated as fresh catalyst, and used in glycerol oxidation in the optimized conditions: the metal loading of Pd/C catalyst was 10 wt% Pd, and of Pt/C catalyst, 5 wt% Pt; the amount of catalyst 0.2–0.8 g; 0.5 M glycerol solution, 0.55 M NaOH, in 100 mL aqueous solution, at 200–230 °C. The most striking conclusion was obtained by the comparison of Pt 4f XPS for the fresh and used Pt/C samples in Fig. 5. Each spectrum in Fig. 5 is composed of a doublet because of spin–orbit coupling in platinum.<sup>47</sup> The lower energy peaks at 72.4 and 71.5 eV in the

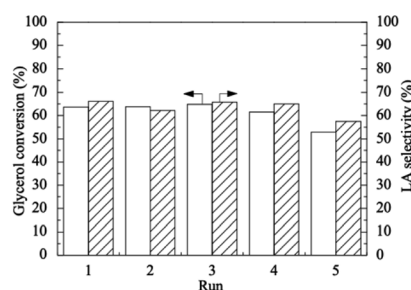


**Fig. 4** (Reproduction of Fig. 3 from ref. 66). The variations in glycerol conversion and LA selectivity in the reusability test of Pt/AC catalyst for glycerol oxidation with an O<sub>2</sub> flow rate of 100 mL min<sup>-1</sup>, glycerol/platinum molar ratio of 2400, LiOH/glycerol molar ratio of 1.5 at 90 °C and 0.1 MPa for 4 h reaction time. Reproduced with permission.<sup>66</sup> Copyright 2016 Elsevier Inc.





spectra of fresh and used samples were assigned to the  $4f_{7/2}$  components of  $Pt^{2+}$  and  $Pt^0$ , respectively.<sup>68</sup> This observation suggests that the platinum species exists as  $Pt^{2+}$  in the fresh sample, which is reduced in the course of glycerol oxidation under reducing conditions at high temperatures.<sup>68</sup> This important conclusion needs to be considered as an example for assigning the active catalyst in glycerol oxidation started with the high oxidation state metal precursors such as metal oxide.<sup>56,58,60</sup> The highest glycerol conversion and LA selectivity obtained for both catalysts under the optimized conditions are given in Table 4. The reusability of both Pd/C and 5% Pt/C catalysts with metal loading of 10% Pd and 5% Pt, respectively, was tested in the glycerol oxidation at a temperature of 230 °C for 3 h whereby the catalyst was isolated after each run by filtration. No significant alteration was observed in glycerol conversion for both catalysts after five successive runs of glycerol oxidation while the LA selectivity slightly changed.<sup>68</sup>

The results of a study on the promoting effect of increasing copper content on the catalytic activity of activated carbon-supported copper-platinum bimetallic catalysts (Cu–Pt/AC) for the glycerol conversion to LA were reported in a 2016 paper by Zhang *et al.*<sup>69</sup> For the preparation of the bimetallic Cu–Pt/AC catalyst, various metal ratios of the copper(II) precursor were impregnated on the surface of activated carbon and first reduced by  $H_2$  at high temperature, and then platinum(0) nanoparticles were deposited by the borohydride reduction of hexachloroplatinic acid onto the surface. Thus, the catalysts were expected to have both metals in the zero oxidation state, as confirmed by XPS. All the catalysts with various compositions were tested in glycerol oxidation under optimized conditions: 25 g glycerol, 0.25 catalyst, LiOH/glycerol ratio of 1.5 in 100 mL aqueous solution with an  $O_2$  flow rate of 100 mL  $min^{-1}$  at 90 °C and 0.1 MPa for 4 h. The results are included in Table 4. The highest TOF value (437  $h^{-1}$ ) for LA formation and glycerol conversion (80%) was obtained by using 0.5%Cu–1.0%Pt/AC catalyst.<sup>69</sup> Unfortunately, the TOF values have not been given

for the 0.35%Cu–1.0%Pt/AC and 0.75%Cu–1.0%Pt/AC catalysts even though the 0.35%Cu–1.0%Pt/AC catalyst provides the highest selectivity to LA (72.9%). A higher copper loading than 0.35% Cu causes a notable gradual decrease in the LA selectivity down to 49.0% for 2.0%Cu–1.0%Pt/AC. Note that all the catalysts have GLYA selectivity higher than 15%, which might be due to low temperature. Copper-promoted platinum(0) supported on activated carbon catalyst<sup>69</sup> exhibited much lower glycerol conversion, but similar LA selectivity (Table 4) as compared to 5% Pt/C.<sup>69</sup> The reusability test was applied on the 0.5%Cu–1.0%Pt/AC. The catalysts were recovered by centrifugation followed by washing with deionized water. Glycerol conversion and LA selectivity maintained the stability for three successive cycles under the same conditions given in Table 4. Since the 1.0%Cu/AC catalyst is not able to convert glycerol under the reaction conditions and the 1.0%Pt/AC catalyst can provide glycerol conversion of 40.6% within 4 h,<sup>69</sup> the coexistence of copper in the bimetallic catalysts plays an important role in the increased catalytic activity for the conversion of glycerol to LA and copper is presumably acting as the promotor. The  $N_2$ -adsorption analysis showed that the Cu-promoted 1.0% Pt/AC catalysts have surface properties such as specific surface area, pore volume, and pore size very similar to those of the unpromoted one. Therefore, the improved catalytic performance of the bimetallic catalysts might be attributed to the intermetallic interactions. However, the collected data, including information obtained by XPS analysis, are insufficient for explaining this anomalous effect.

#### 4. Other catalysts

The effect of bentonite-supported gold nanoparticles on the conversion of glycerol to LA was studied by Sever and Yildiz<sup>70</sup> in the presence of a base. Selectivity towards LA was enhanced upon the catalyst reduction. However, no significant difference between the effects of reduced and unreduced catalysts on the conversion of glycerol was detected. Additional oxygen flow led to an increase in glycerol conversion while causing a significant decrease in the selectivity to LA. The effect of increasing the molar ratio of catalyst to glycerol was also investigated on the conversion of glycerol to LA. The optimized selectivity (92.3%) to LA was achieved using 0.25 g of 1 wt% Au/bentonite catalyst after 240 min. The conversion of glycerol soared up to nearly 90%, but selectivity for LA dropped to almost 40% upon increasing the amount of catalyst from 0.25 g to 0.7 g. The reaction was also carried out in the presence of different bases with 1 wt% Au/bentonite catalyst. The maximum selectivity for LA was obtained using NaOH although LiOH and KOH led to higher conversion of glycerol.

Two copper oxides (CuO and  $Cu_2O$ ) and six copper salts ( $CuBr_2$ , CuBr,  $CuCl_2$ , CuCl,  $CuF_2$ , and  $Cu(NO_3)_2$ ) were tested in the conversion of glycerol to LA in an aqueous NaOH solution.<sup>71</sup> For halogenated copper compounds, the decreasing order of glycerol conversion and LA yield is Br > Cl > F (Fig. 2 in that paper).<sup>71</sup>  $Cu(NO_3)_2$  had the lowest glycerol conversion with LA yield among the copper compounds. Copper(II) species also showed higher conversion of glycerol with LA yields as

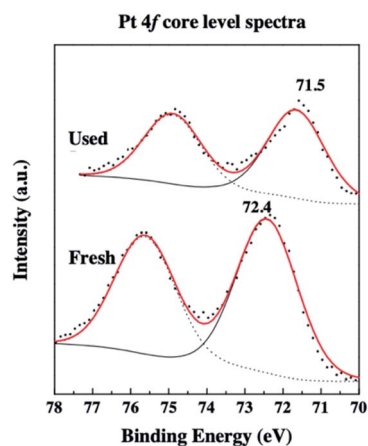


Fig. 5 (Reproduction of Fig. 5b from ref. 68). High-resolution scan Pt 4f core-level XPS for Pt/C-nanoparticles, before (fresh) and after (used) catalytic glycerol oxidation. Reproduced with permission.<sup>68</sup> Copyright 2017 Elsevier Inc.



compared to copper(i) species. The effect of temperature on glycerol conversion and LA yield for the reactions carried out using CuBr<sub>2</sub> and CuO as catalysts were demonstrated in Fig. 4 of that paper<sup>71</sup> with a molar ratio of NaOH/glycerol 1.5 for 4 h. At 185 °C, 98.7% conversion of glycerol and 95.7% yield of LA were achieved upon CuBr<sub>2</sub>.

## 5. Catalysts in the conversion of glycerol to LA in the absence of a base

Although it has already been shown that the presence of 1 equivalent of base per mole of glycerol is necessary for the oxidation of glycerol in the absence or presence of catalyst,<sup>24,66</sup> there are reports of catalysts that can accelerate the rate of glycerol oxidation without any added base.<sup>72–74</sup> We will also inevitably review all the papers claiming the achievement of the catalytic glycerol conversion to LA without adding any base. A 2011 paper<sup>75</sup> reported the conversion of pure and crude glycerol obtained from the transesterification of rapeseed oil to LA using sodium silicate as a catalyst. The sodium silicate appeared to catalyse the transesterification of oil and subsequently the conversion of crude glycerol to LA at 300 °C.<sup>75</sup> Unfortunately, the Brønsted basicity of sodium silicate was not taken into account in that paper.<sup>75</sup>

A 2014 paper<sup>76</sup> covered the catalytic performance of zeolite-supported Au–Pt nanoparticles for the conversion of glycerol to LA without using a base in the presence of molecular oxygen. Bimetallic Au–Pt nanoparticles were supported on different acidic zeolites and tested for the conversion of glycerol to LA at 140 and 180 °C for 2 h in aqueous media with 3 bar pressure of O<sub>2</sub>. Although some conversion of glycerol was obtained, the acidic and basic properties of zeolites have not been explored for the oxidation.

The article by Wang *et al.*<sup>77</sup> indicated the catalytic conversion of glycerol to LA by H<sub>3</sub>PMo<sub>12</sub>O<sub>40</sub> (HPMo) and H<sub>3</sub>PMo<sub>12</sub>O<sub>40</sub> on a carbon support (HPMo/C) under mild base-free conditions. Due to the lipid-like structure of carbon-supported heteropolyacids (HPA), glycerol and oxygen molecules were adsorbed on the surface of HPMo and HPMo/C enabled the transformation of glycerol to LA. The significantly higher adsorption of both glycerol and oxygen was detected on the surface of HPMo/C as compared to HPMo.<sup>77</sup> The optimized selectivity for LA using HPMo/C was obtained at 60 °C, and selectivity started to gradually decrease upon increasing the reaction temperature to 90 °C. The optimal weight ratio of glycerol to HPMo/C was detected as 10 : 1 for complete conversion to LA after 5 h. Lowering the amount of catalyst caused the incomplete conversion of intermediates.<sup>77</sup> On the other hand, increasing the amount of catalyst or reaction time did not affect the selectivity of LA. In order to achieve the complete conversion of glycerol, 30 wt% HPMo/C was required. HPMo/C also exhibited the same conversion (98%) for crude glycerol and selectivity (90%) to LA. Additionally, HPMo/C was reused five times with a small loss in catalytic activity.<sup>77</sup> In contrast to the claim that the catalytic conversion would occur under base-free conditions, no control experiments have been performed with a strong base.<sup>77</sup>

Another paper by Wang *et al.*<sup>78</sup> reported the usage of polyoxometalates AlPMo<sub>12</sub>O<sub>14</sub> and CrPMo<sub>12</sub>O<sub>40</sub> as heterogeneous catalysts for glycerol conversion to LA under ostensibly base-free conditions. The catalysts consisted of the Lewis acid side with Al<sup>3+</sup> or Cr<sup>3+</sup>, and the redox core PMo<sub>12</sub>O<sub>40</sub>. AlPMo<sub>12</sub>O<sub>14</sub> and CrPMo<sub>12</sub>O<sub>40</sub> provided 93.7% and 88.0% glycerol conversion, and 90.5% and 80.3% LA selectivity, respectively, at 60 °C for 5 h. However, TOF values for AlPMo<sub>12</sub>O<sub>14</sub> and CrPMo<sub>12</sub>O<sub>40</sub> were just 41.5 and 31.7 h<sup>-1</sup> at 60 °C under a pressure of 10 bar. Both catalysts could be reused with 93.7% glycerol conversion, and 90.5% LA selectivity for more than twelve cycles. Although no base was added to the reactor, the pH of the reaction solution was not checked. The same research group also investigated the effect of silver-exchanged phosphomolybdic acid catalysts (Ag<sub>x</sub>H<sub>3–x</sub>PMo<sub>12</sub>O<sub>40</sub>, *x* = 1–3) on the conversion of glycerol to LA using O<sub>2</sub> as an oxidant under base-free conditions.<sup>79</sup> However, the pH of the reaction solution was not measured either.

A 2020 paper by Wang *et al.*<sup>80</sup> reported the use of another polyoxometalate-based catalyst for glycerol conversion to LA without an additional base. Lysine-functionalized phosphomolybdic acids with the coexistence of the basic side, Brønsted acidic side, and the redox core with different compositions (Ly<sub>x</sub>H<sub>3–x</sub>PMo, *x* = 1–3) have been tested for the oxidation of glycerol to LA at 80 °C for 3 h in the presence of 1 MPa of O<sub>2</sub>. Higher catalytic activities were observed for the amino acid-functionalized polyoxometalate as compared to AlPMo<sub>12</sub>O<sub>14</sub> and CrPMo<sub>12</sub>O<sub>40</sub>, and Ag<sub>x</sub>H<sub>3–x</sub>PMo<sub>12</sub>O<sub>40</sub>.<sup>78–80</sup> The highest LA selectivity of 38% was obtained by Ly<sub>2</sub>H<sub>1</sub>PMo. However, no control experiment has been performed to determine how the addition of a base or changing the pH would have affected the kinetics of the glycerol conversion.<sup>80</sup>

A 2017 paper by Wang *et al.*<sup>81</sup> reported the use of a composite HPMo@lipid(*n*)/GO consisting of heteropolyacids embedded in a lipid-like bilayer *a*-NH-(CH<sub>2</sub>)<sub>2</sub>-NH<sub>2</sub><sup>+</sup>-CH<sub>2</sub>(CH<sub>2</sub>)<sub>*n*</sub>CH<sub>3</sub> with different lengths of diamine carbon chain covalently bonded to graphene oxide as the catalyst for glycerol conversion to LA in the absence of additional base. The highest catalytic activity (TOF = 258 h<sup>-1</sup>) was obtained with an almost complete conversion of glycerol and LA selectivity of 93% by using HPMo@lipid(4)/GO at 60 °C and 10 bar of O<sub>2</sub> for 3.5 h. However, the pH of the reaction solution has not been investigated.<sup>81</sup>

A bifunctional catalyst consisting of platinum nanoparticles and layered-Nb<sub>2</sub>O<sub>5</sub> (L-Nb<sub>2</sub>O<sub>5</sub>) was reported to efficiently catalyse the one-pot conversion of glycerol to LA in water under an oxygen atmosphere without the use of any additives such as strong bases.<sup>82</sup> Mechanistic studies revealed that glycerol was initially oxidized to DHA and GAL through dehydrogenation on platinum nanoparticles.<sup>82</sup> After the dehydration step catalysed by acid sites on L-Nb<sub>2</sub>O<sub>5</sub>, the dehydrated intermediate pyruvic aldehyde was converted exclusively on Lewis acid sites rather than Brønsted acid to produce LA through the Cannizzaro reaction. These experimental results presented the successful development of a binary catalyst consisting of metal NPs and solid acid, Pt/L-Nb<sub>2</sub>O<sub>5</sub>, for the one-pot synthesis of LA from glycerol under additive-free conditions. However, the Brønsted basicity of the materials has not been investigated.<sup>82</sup>



The catalytic conversion of glycerol to LA under base-free conditions has been mostly studied using oxygen as an oxidative reagent. The molecular oxygen has an active role in the first step of the reaction, which is the oxidation of glycerol to GAL or DHA. The catalyst amino acid-functionalized polyoxometalates include both acidic and basic sites. The basic and acidic sites presumably catalysed the dehydration of GAL or DHA to PAL and conversion of PAL to LA, respectively.<sup>80</sup> The generation of LA from the intermediate PAL is accelerated more in the presence of Lewis acid sites rather than the Brønsted acid ones.<sup>79</sup> The catalysts in studies of glycerol conversion to LA without an additive base do not show catalytic activity that is as high as that in basic solution. More importantly, the effect of added strong base has never been investigated in those works claiming to achieve the catalytic conversion of glycerol without additional base.

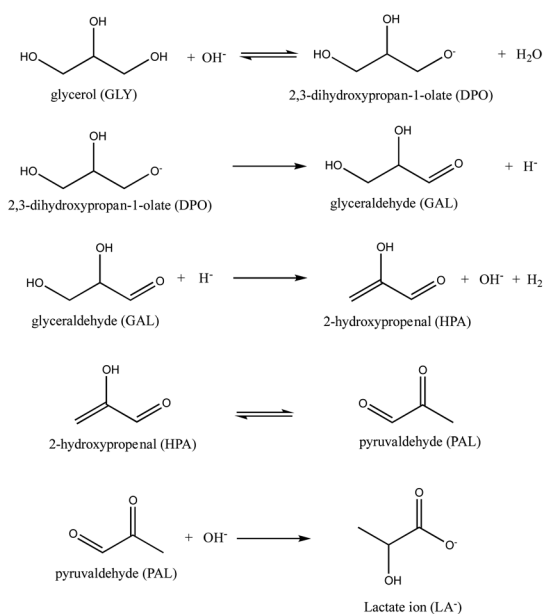
## 6. Mechanisms

The conversion of glycerol to LA in the absence of a catalyst has been studied in an alkaline solution by Emenoto *et al.*<sup>83</sup> The reaction was performed in a nitrogen-purged reactor starting with an aqueous solution of 0.33 M glycerol and 0.25–1.25 M NaOH at 300 °C and followed by HPLC and GC.<sup>83</sup> Based on the experimental observations, a plausible mechanism was proposed for the conversion of glycerol to LA in the absence of catalyst (Scheme 1).<sup>83</sup> The mechanism consists of five steps that sum up to the stoichiometric reaction in eqn (1). In the first step, the deprotonation of one of the terminal hydroxyl groups of glycerol (GLY) produces the glycerol alkoxide (DPO) and water because glycerol has a  $pK_a$  of 14.4.<sup>84</sup> In the second step, the glycerol alkoxide (DPO) loses a hydride ion to form glyceraldehyde (GAL). The third step is the dehydration in the  $E_2$

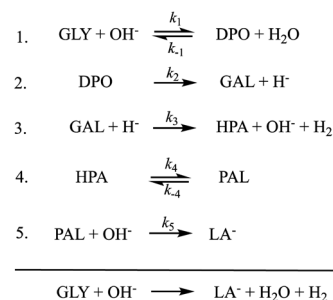
mechanism through  $\alpha$ -proton abstraction by the hydride ion releasing  $H_2$  gas and forming 2-hydroxypropenal (HPA). In the fourth step, HPA undergoes keto–enol tautomerization resulting in the formation of pyruvaldehyde (PAL). The final step is the formation of the lactate ion through the benzylic acid rearrangement of PAL.<sup>85</sup>

The paper by Emenoto *et al.*<sup>83</sup> also provides excellent kinetics data obtained by HPLC and GC analysis for the conversion of glycerol to LA in a basic medium without the addition of catalysts (Fig. 4 of that paper). Surprisingly, these excellent kinetics data have not been fit to the mechanism in Scheme 1. Fortunately, we were able to curve-fit the kinetics data to the 5-step mechanism concisely described in Scheme 2. The COPASI 4.19 (Build 140) software<sup>86</sup> was used for curve-fitting the kinetics data to the 5-step mechanism in Scheme 2 using the particle swarm method with an iteration limit of 5000 and a swarm size of 1000 with bounds of 0–1000. Fig. 6 demonstrates that the kinetics data in Fig. 4 of that paper fit very well with the 5-step mechanism in Scheme 2. The respective rate constants for the individual steps of the 5-step mechanism obtained from the curve-fitting are also given in the Fig. 6 caption. The most important finding obtained from the fitting of the kinetics data is that the concentration of the glycerol alkoxide (DPO) intermediate remains very low ( $[DPO] < 0.01$  M) during the glycerol  $\rightarrow$  LA conversion. This observation leads to the conclusion that the rate-determining step in the production of LA from glycerol is the second step, *i.e.*, the formation of GAL from DPO. The mechanism in Scheme 1 proposed by Emenoto *et al.*<sup>83</sup> for the glycerol conversion to lactate ion in the presence of base has also been supported by a relatively recent paper by Zavrzhnov *et al.*<sup>87</sup> However, one problem in the mechanism given in Scheme 3 of that paper<sup>87</sup> is the release of the proton during the formation of GAL instead of a hydride ion. Note that such a reversible release of a proton is unlikely in a basic medium. The mechanism in the 2018 paper<sup>87</sup> has been extended to explain all the side products.<sup>88</sup>

Scheme 3 shows the mechanism proposed for the conversion of glycerol to LA in the presence of soluble iridium complexes,<sup>20</sup> with a small modification of changing the LA to the lactate ion as the reaction is performed in a basic medium. The mechanism in Scheme 3 is essentially similar to the one in Scheme 1, with a few differences. One difference is the consideration of an



**Scheme 1** The mechanism proposed for the conversion of glycerol to the lactate anion in alkaline solution in the absence of a catalyst.<sup>83</sup>



**Scheme 2** The 5-step mechanism proposed for the conversion of glycerol to lactate anion in alkaline solution in the absence of a catalyst.<sup>85</sup>



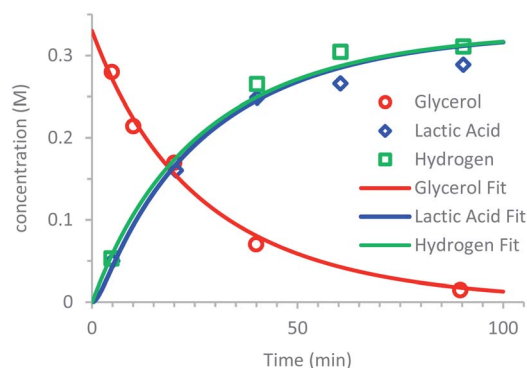
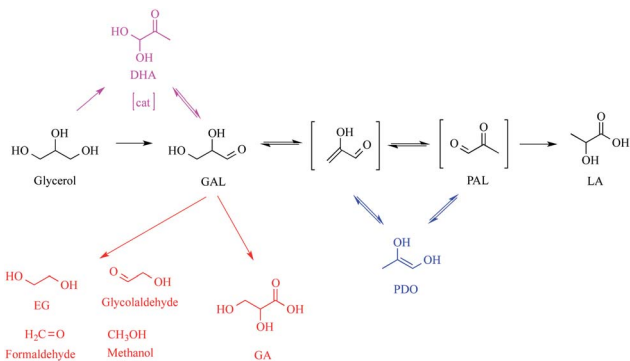


**Fig. 6** Curve-fitting of the kinetics data for the conversion of glycerol to the lactate anion in alkaline solution in the absence of catalyst at 300 °C from Fig. 4 of the ref. 83 to the 5-step mechanism in Scheme 2. COPASI curve fitting yields the rate constants for the five steps:  $k_1 = 3.2 \times 10^{-2} \text{ M}^{-1} \text{ min}^{-1}$ ,  $k_{-1} = 7.9 \times 10^1 \text{ min}^{-1}$ ,  $k_2 = 3.5 \times 10^{-2} \text{ min}^{-1}$ ,  $k_3 = 4.1 \times 10^{-1} \text{ M}^{-1} \text{ min}^{-1}$ ,  $k_4 = 6.8 \times 10^1 \text{ min}^{-1}$ ,  $k_{-4} = 1.7 \times 10^{-2} \text{ min}^{-1}$ ,  $k_5 = 5.9 \times 10^{-2} \text{ M}^{-1} \text{ min}^{-1}$ .

additional alternative catalytic pathway to the rate-determining step, which proceeds through dihydroxyacetone (DHA). It has been shown that starting the reaction with DHA gives a higher yield for GAL.<sup>89,90</sup> Thus, the formation of GAL is accelerated by the iridium catalyst. Another difference of this mechanism from the one in Scheme 1 is the addition of three pathways for the formation of additional side-products observed for the reaction in the presence of iridium catalyst. In the second step, the base-catalysed dehydration of GAL generates PAL, which is converted to LA by an intramolecular Cannizzaro reaction. Although the proposed mechanism in Scheme 3 doesn't explain how the iridium complex is involved in the catalysis, its use presumably minimizes the formation of side products such as formaldehyde or EG.<sup>19</sup> Since the reduction is reversible and the formation of LA is irreversible, the use of iridium complexes as catalysts presumably provides high selectivity for LA. An important conclusion given in the 2014 article<sup>19</sup> is that the purification of crude glycerol obtained from industrial waste is



**Scheme 3** The mechanism for the conversion of glycerol to LA in the presence of homogeneous catalysts in a basic medium, adapted from the mechanism given in the 2014 paper.<sup>20</sup> DHA: dihydroxyacetone; GAL: glyceraldehyde; EG: ethylene glycol; GA: glyceric acid; PDO: 1,2-propanediol; PAL: pyruvaldehyde.

not required for its catalytic conversion to LA by following the given catalytic process. The same mechanism was propounded by Shen *et al.*<sup>65</sup> and Li *et al.*<sup>63</sup> for the catalytic conversion of glycerol to LA using the Ni/graphite<sup>65</sup> and Cu–Zn–Al<sup>63</sup> catalysts, respectively. Although the 2018 paper<sup>87</sup> has reported a mechanism for the uncatalyzed glycerol conversion to LA in the basic medium, which is essentially consistent with the mechanism in Scheme 1, the mechanism proposed for the catalytic conversion of glycerol to LA (Scheme 6 of that paper<sup>87</sup>) appears not to be plausible as the catalyst has been used in the steps which are not the rate-determining steps.

The mechanism in Scheme 3 has been supported by the results reported in two papers on the glycerol to LA conversion in the presence of homogeneous iridium complexes by Williams *et al.*<sup>21</sup> and Dutta *et al.*<sup>22</sup> A similar mechanism has been proposed for the glycerol conversion to LA in a basic medium in the presence of heterogeneous copper-based catalysts,<sup>56</sup> where the first step is the dehydrogenation of glycerol to form GAL and the second step is the dehydration of GAL, resulting in the formation of 2-hydroxypropanal. Then, 2-hydroxypropanal undergoes keto–enol tautomerization and is converted to PAL followed by benzylic acid rearrangement (see Scheme 1 in that paper).<sup>56</sup> PAL was observed as a side product in the reactions carried out using Cu/SiO<sub>2</sub> and CuO/Al<sub>2</sub>O<sub>3</sub>, but it was not observed while using Cu<sub>2</sub>O as the catalyst.<sup>56</sup> An increase in the formation of PDO as a side-product was seen in the reactions catalysed by Cu<sub>2</sub>O. The side-products were GAL, EG, AA, FA, and ethanol in trace amounts, except that methanol was formed with 5.15% selectivity when Cu/SiO<sub>2</sub> was used.<sup>56</sup> A major flaw of this mechanism is that how and in which step the active catalyst would be involved in the whole set of pathways have not been investigated.<sup>56</sup> Nevertheless, the mechanism has also been adopted for the copper-catalysed conversion of glycerol to LA in alkaline solution as reported in two papers by Manfro *et al.*,<sup>28,60</sup> as well as for the catalytic conversion of glycerol to LA in the presence of heterogeneous Ru–Zn–Cu(I)/HAP catalyst reported by Han *et al.*<sup>32</sup> In the latter mechanism, the first step is again the dehydrogenation of glycerol to GAL, which is followed by the dehydration of GAL to form PAL, and the presence of Zn<sup>2+</sup> ions is assumed to promote the 1,2-hydride shift in PAL forming LA.<sup>32</sup> It was observed that introducing the copper(I) significantly decreased FA formation.<sup>32</sup> A 2017 paper by Vieira *et al.*<sup>68</sup> reported the use of a similar mechanism for the glycerol conversion catalysed by carbon-supported palladium or platinum nanoparticles. The only difference from the mechanism in Scheme 3 is the assumption of equilibrium between DHP and GAL after the catalytic oxidative dehydrogenation of glycerol. Further oxidation of DHA leads to the formation of glycolic acid and FA while dehydration of GAL can result in the formation of LA as the ultimate product (see Fig. 6 of that paper<sup>68</sup>). The paper by Ding *et al.*<sup>69</sup> also reported the consideration of a similar equilibrium between GAL and DHP after the oxidation of glycerol catalysed by the carbon-supported copper–platinum catalysts. However, different from the 2017 paper by Vieira *et al.*,<sup>68</sup> it reports that the use of Cu<sup>+</sup> and Cu<sup>0</sup> as promoters leads to the conversion of DHA to LA as the ultimate product, while the use of a large amount of CuO as promoter results in the conversion





of GAL to GA as the side-product.<sup>69</sup> A 2019 paper by Shen *et al.*<sup>19</sup> reported that bimetallic CuPd<sub>x</sub> nanoparticles catalyse the oxidation of glycerol to GAL, which can ultimately produce LA in the basic medium. The same mechanism has been adopted to explain the catalytic activity of Cu<sub>2</sub>O nanoparticles,<sup>54</sup> graphite-supported Ni nanoparticles,<sup>65</sup> and NiO<sub>x</sub> nanocatalyst<sup>64</sup> in the oxidation of glycerol to GAL, while the formation of side products has been explained by considering different pathways.

## 7. Concluding remarks and a look towards future research

The review of papers on the glycerol oxidation to LA in aqueous alkaline solution has yielded the following conclusions and suggestions for future research:

- The development of high-activity catalysts for selective glycerol conversion to LA without significant side products is still a paramount challenge due to the important transformation of the rapidly increasing amount of biodiesel by-product into a potential starting chemical in the food, pharmaceutical, and cosmetic industries.

- The developed catalysts are usually found to be applicable to the crude glycerol to avoid additional purification steps before its conversion to LA.

- The oxidation of glycerol to LA negligibly occurs in the absence of catalysts in alkaline solution, at least at moderate temperatures. Although the catalytic conversion of glycerol to LA has been claimed to occur without adding a strong base such as sodium hydroxide in a few studies, the basicity of the medium has been underestimated in those studies. Thus, one can conclude that both a suitable catalyst and a strong base need to be inevitably used for achieving a notable glycerol conversion to LA at temperatures lower than 200 °C.

- In general, sodium hydroxide is used as a strong Brønsted base in aqueous solution for the catalytic glycerol conversion, and usually at least 1 equivalent NaOH per mole of glycerol is needed.

- It needs to be noted that none of the papers, reviewed herein, have reported the actual *E* factor (environmental factor)<sup>91</sup> for the conversion of glycerol to lactic acid. A theoretical *E* factor of 47 kg waste per kg of lactic acid was calculated for the conversion of glycerol to lactic acid, assuming (i) 100% chemical yield, (ii) no loss of catalyst, and (iii) exactly stoichiometric quantities of the various reagents such as sodium hydroxide. The obvious challenge is to lower the *E* factor for this industrially important process, which seems to be tough as long as the conversion is carried out in the presence of an aqueous base.

- Homogeneous catalysts show in general higher catalytic activity than heterogeneous materials in the glycerol conversion to LA. However, the major drawback of homogeneous catalysts is their miserable recovery from the reaction solution, which makes them not reusable.

- Heterogeneous catalysts are mainly considered to be used in glycerol conversion to LA, most likely because of their easy recovery and preparation as compared to homogeneous catalysts.

- As hybrid catalysts, colloidal nanoparticles of transition metals are expected to play an important role in catalysing the glycerol conversion to LA. Unfortunately, there exists only one example of using colloidal metal nanoparticles as catalysts for glycerol conversion;<sup>19</sup> namely, the PEG-stabilized bimetallic copper(0)–palladium(0) nanoparticles are found to be highly active catalysts providing the highest glycerol conversion at 180 °C. However, the use of colloidal metal(0) nanoparticles as catalysts in glycerol oxidation has not been further explored, likely due to their instability against agglomeration, particularly at high temperatures. Further research is needed to stabilize metal nanoparticles in basic solution at temperatures as high as 200 °C for use as catalysts in the selective conversion of glycerol to LA.

- The oxide-supported metal(0) nanoparticles show decent activity in the oxidation of glycerol to LA in alkaline solution. However, the limited surface area of oxide supports restricts the catalytic activity of the supported metal nanoparticles.

- Hydroxyapatite (HAP) appears to be a promising support, particularly for non-noble metal(0) nanoparticles such as copper and nickel. Thus, the HAP-supported nickel and copper nanoparticles provide high glycerol conversion and high selectivity for LA at moderate temperatures. Consequently, HAP is suggested for exploration as a support for the other non-noble metal catalysts in the oxidation of glycerol to LA.

- The noble metals such as platinum and gold expectedly provide high catalytic activity for glycerol oxidation as well. For example, zirconia-supported platinum(0) nanoparticles provide the highest activity of TOF = 995 h<sup>-1</sup> for the selective conversion of glycerol to LA at a low temperature (160 °C). However, this precious metal nanocatalyst was found to have very low reusability.<sup>34</sup> The challenge would be making the high-activity precious metal nanoparticles a reusable nanocatalyst for the selective conversion of glycerol to LA, for example, by supporting them on magnetic nanopowders.<sup>92</sup>

- The use of reducible oxide titania as a support seems to be a suitable method for increasing the catalytic activity of gold and platinum nanoparticles or their bimetallic alloys in glycerol oxidation to LA at low temperature.<sup>43</sup> The titania-supported gold–platinum nanocatalysts need to be optimized to increase the catalytic performance and utilization efficiency in the glycerol conversion to LA at temperatures as low as possible. Other reducible oxides that have already been shown to provide favourable metal–support interaction, particularly for platinum(0) nanoparticles<sup>50,93–95</sup> should also be investigated as catalyst supports for the glycerol conversion.

- Reducible copper oxide appears to be a cost-effective catalyst for glycerol oxidation to LA.<sup>28</sup> For example, the CuO/ZrO<sub>2</sub> catalyst exhibited the highest glycerol conversion (100%) and selectivity for LA (94.6%) at 180 °C under an inert atmosphere.<sup>57</sup> Further improving the copper-based catalysts is a challenge in the selective glycerol conversion to LA and an interesting subject for future studies.

- In using the multimetallic ruthenium nanoparticles such as Ru–Zn–Cu/HAP in glycerol oxidation,<sup>32</sup> a problem arises since ruthenium enables the cleavage of C–C bonds in hydrocarbons and causes the degradation of LA to FA, resulting inevitably in



the formation of methane and carbon dioxide. Hence, one has to be careful as the ruthenium component would lower the selectivity to LA while the other components of multimetallic nanoparticles may give a high glycerol conversion.

- Carbonaceous materials have been used as supports for the transition metal nanoparticles in glycerol oxidation to LA. The carbon-<sup>64</sup> and graphite<sup>65</sup>-supported nickel nanoparticles have been shown to provide high catalytic activity in the glycerol conversion to LA (Table 4). Additionally, the intrinsically magnetic nickel(0) nanoparticles can be isolated using an external magnet, and therefore, they are highly reusable catalysts.

- Most of the studies on the catalysts for glycerol conversion to LA without an additive base involve oxygen as an oxidant that can oxidize glycerol to GAL or DHA. The catalysts, except for the paper using sodium silicate as a catalyst,<sup>75</sup> presumably contain acidic sites that are effective in the last step, the conversion of PAL to LA. Lewis acid sites are more favourable than Brønsted acid sites for that step.<sup>79</sup> More importantly, the effect of added strong base has never been investigated in those works claiming to achieve the catalytic conversion of glycerol without an additional base.

- Plausible mechanisms exist for the conversion of glycerol to LA in the presence of homogeneous and heterogeneous catalysts in an aqueous alkaline solution. Fitting the available kinetics data to the proposed mechanism indicates that the rate-determining step is the oxidation of glycerol to GAL. This rate-determining step is accelerated by the catalysts.

## Author contributions

Authors have contributed equally.

## Conflicts of interest

There are no conflicts to declare.

## Acknowledgements

Partial support by Turkish Academy of Sciences is gratefully acknowledged.

## Notes and references

- 1 S. M. Ameen and G. Caruso, *Lactic Acid in the Food Industry*, SpringerBriefs in Molecular Science, Cham, Switzerland, 2017.
- 2 P. Saini, M. Arora and M. N. V. R. Kumar, *Adv. Drug Delivery Rev.*, 2016, **107**, 47–59.
- 3 W. P. Smith, *J. Am. Acad. Dermatol.*, 1996, **35**, 388–391.
- 4 N. Madnani and K. Khan, *Indian J. Dermatol. Venereol.*, 2013, **79**, 654–667.
- 5 M. Ai and K. Ohdan, *Appl. Catal., A*, 1997, **150**, 13–20.
- 6 V. C. Ghantani, S. T. Lomate, M. K. Dongare and S. B. Umbarkar, *Green Chem.*, 2013, **15**, 1211–1217.
- 7 X. Li, Z. Zhai, C. Tang, L. Sun, Y. Zhang and W. Bai, *RSC Adv.*, 2016, **6**, 62252–62262.
- 8 S. Liu, H. Feng, T. Li, Y. Wang, N. Rong and W. Yang, *Green Chem.*, 2020, **22**, 7468–7475.
- 9 B. Katryniok, S. Paul and F. Dumeignil, *Green Chem.*, 2010, **12**, 1910–1913.
- 10 Y. Wang, S. Furukawa, S. Song, Q. He, H. Asakura and N. Yan, *Angew. Chem., Int. Ed.*, 2020, **132**, 2309–2313.
- 11 X. Su, W. Lin, H. Cheng, C. Zhang, Y. Wang, X. Yu, Z. Wu and F. Zhao, *Green Chem.*, 2017, **19**, 1775–1781.
- 12 V. Bhardwaj, K. Sharma, S. Maksimovic, A. Fan, A. Adams-Woodford and J. Mao, *Front. Med.*, 2021, **8**, e617068.
- 13 A. H. Somro, T. Masud and K. Anwaar, *Pak. J. Nutr.*, 2001, **1**, 20–24.
- 14 M. R. Monteiro, C. L. Kugelmeier, R. S. Pinheiro, M. O. Batalha and A. da Silva César, *Renewable Sustainable Energy Rev.*, 2018, **88**, 109–122.
- 15 X. Chen, S. Song, H. Li, G. Gözaydin and N. Yan, *Acc. Chem. Res.*, 2021, **54**, 1711–1722.
- 16 N. Yan and X. Chen, *Nature*, 2015, **524**, 155–157.
- 17 T. Zhang, *Science*, 2020, **367**, 1305–1306.
- 18 X. Wang, Y. Song, C. Huang, F. Liang and B. Chen, *Green Chem.*, 2014, **16**, 4234–4240.
- 19 L. Shen, X. Zhou, C. Zhang, H. Yin, A. Wang and C. Wang, *J. Food Biochem.*, 2019, **43**, e13061.
- 20 L. S. Sharninghausen, J. Campos, M. G. Manas and R. H. Crabtree, *Nat. Commun.*, 2014, **5**, e5084.
- 21 Z. Lu, I. Demianets, R. Hamze, N. J. Terrile and T. J. Williams, *ACS Catal.*, 2016, **6**, 2014–2017.
- 22 M. Dutta, K. Das, S. J. Prathapa, H. K. Srivastava and A. Kumar, *Chem. Commun.*, 2020, **56**, 9886–9889.
- 23 M. Finn, J. A. Ridenour, J. Heltzel, C. Cahill and A. Voutchkova-Kostal, *Organometallics*, 2018, **37**, 1400–1409.
- 24 L. Chen, S. Ren and X. P. Ye, *React. Kinet., Mech. Catal.*, 2014, **114**, 93–108.
- 25 C. A. Ramírez-López, J. R. Ochoa-Gómez, M. Fernández-Santos, O. Gómez-Jimenez-Aberasturi, A. Alonso-Vicario and J. Torrecilla-Soria, *Ind. Eng. Chem. Res.*, 2010, **49**, 6270–6278.
- 26 S. Özkar, *Appl. Surf. Sci.*, 2009, **256**, 1272–1277.
- 27 H. Yin, C. Zhang, H. Yin, D. Gao, L. Shen and A. Wang, *Chem. Eng. J.*, 2016, **288**, 332–343.
- 28 A. B. F. Moreira, A. M. Bruno, M. M. V. M. Souza and R. L. Manfro, *Fuel Process. Technol.*, 2016, **144**, 170–180.
- 29 A. M. Bruno, C. A. Chagas, M. M. V. M. Souza and R. L. Manfro, *Renewable Energy*, 2018, **118**, 160–171.
- 30 Z. Tang, P. Liu, H. Cao, S. Bals, H. J. Heeres and P. P. Pescarmona, *ACS Catal.*, 2019, **9**, 9953–9963.
- 31 L. Shen, Z. Yu, D. Zhang, H. Yin, C. Wang and A. Wang, *J. Chem. Technol. Biotechnol.*, 2019, **94**, 204–215.
- 32 Z. Jiang, Z. Zhang, T. Wu, P. Zhang, J. Song, C. Xie and B. Han, *Chem.-Asian J.*, 2017, **12**, 1598–1604.
- 33 L. Qiu, H. Yin, H. Yin and A. Wang, *J. Nanosci. Nanotechnol.*, 2018, **18**, 4734–4745.
- 34 J. Ftouni, N. Villandier, F. Auneau, M. Besson, L. Djakovitch and C. Pinel, *Catal. Today*, 2015, **257**, 267–273.
- 35 R. Palacio, D. López and D. Hernández, *J. Nanopart. Res.*, 2019, **21**, e148.



- 36 S. Duman and S. Özkar, *Int. J. Hydrogen Energy*, 2018, **43**, 15262–15274.
- 37 S. Tanyıldızı, I. Morkan and S. Özkar, *Mol. Catal.*, 2017, **434**, 57–68.
- 38 D. Özhava and S. Özkar, *Appl. Catal., B*, 2018, **237**, 1012–1020.
- 39 E. Demir, S. Akbayrak, A. M. Önal and S. Özkar, *ACS Appl. Mater. Interfaces*, 2018, **10**, 6299–6308.
- 40 S. Karaboga and S. Özkar, *Int. J. Hydrogen Energy*, 2019, **44**, 26296–26307.
- 41 S. Akbayrak, Y. Tonbul and S. Özkar, *Appl. Catal., B*, 2017, **206**, 384–392.
- 42 P. Lakshmanan, P. P. Upare, N.-T. Le, Y. K. Hwang, D. W. Hwang, U. H. Lee, H. R. Kim and J.-S. Chang, *Appl. Catal., A*, 2013, **468**, 260–268.
- 43 Y. Shen, S. Zhang, H. Li, Y. Ren and H. Liu, *Chem.–Eur. J.*, 2010, **16**, 7368–7371.
- 44 H. Lang, S. Maldonado, K. J. Stevenson and B. D. Chandler, *J. Am. Chem. Soc.*, 2004, **126**, 12949–12956.
- 45 D. Mott, J. Luo, P. N. Njoki, Y. Lin, L. Wang and C. Zhong, *Catal. Today*, 2007, **122**, 378–385.
- 46 H. Tada, F. Suzuki, S. Ito, T. Akita, K. Tanaka, T. Kawahara and H. Kobayoshi, *J. Phys. Chem. B*, 2002, **106**, 8714–8720.
- 47 J. R. Croy, S. Mostafa, L. Hickman, H. Heinrich and B. R. Cuenya, *Appl. Catal., A*, 2008, **350**, 207–216.
- 48 S. Özkar, *Dalton Trans.*, 2021, **50**, 12349–12364.
- 49 Y. Li, S. Chen, J. Xu, H. Zhang, Y. Zhao, Y. Wang and Z. Liu, *Clean*, 2014, **42**, 1140–1144.
- 50 R. K. P. Purushothaman, J. van Haveren, D. S. van Es, I. Melián-Cabrera, J. D. Meeldijk and H. J. Heeres, *Appl. Catal., B*, 2014, **147**, 92–100.
- 51 S. Wang, K. Yin, Y. Zhang and H. Liu, *ACS Catal.*, 2013, **3**, 2112–2121.
- 52 F. Cai, W. Zhu and G. Xiao, *Catal. Sci. Technol.*, 2016, **6**, 4889–4900.
- 53 C. Wang, X. Zhang, J. Li, X. Qi, Z. Guo, H. Wei and H. Chu, *ACS Appl. Mater. Interfaces*, 2021, **13**, 522–530.
- 54 L. Shen, H. Yin, H. Yin, S. Liu and A. Wang, *J. Nanosci. Nanotechnol.*, 2017, **17**, 780–787.
- 55 H. Yin, H. Yin, A. Wang, L. Shen, Y. Liu and Y. Zheng, *J. Nanosci. Nanotechnol.*, 2017, **17**, 1255–1266.
- 56 D. Roy, B. Subramaniam and R. V. Chaudhari, *ACS Catal.*, 2011, **1**, 548–551.
- 57 G.-Y. Yang, Y.-H. Ke, H.-F. Ren, C.-L. Liu, R.-Z. Yang and W.-S. Dong, *Chem. Eng. J.*, 2016, **283**, 759–767.
- 58 R. Palacio, S. Torres, S. Royer, A. S. Mamede, D. López and D. Hernández, *Dalton Trans.*, 2018, **47**, 4572–4582.
- 59 R. Palacio, S. Torres, D. Lopez and D. Hernandez, *Catal. Today*, 2018, **302**, 196–202.
- 60 A. M. Bruno, T. D. R. Simões, M. M. V. M. Souza and R. L. Manfro, *RSC Adv.*, 2020, **10**, 31123–31138.
- 61 T. Shimanouchi, S. Ueno, K. Shidahara and Y. Kimura, *Chem. Lett.*, 2014, **43**, 535–537.
- 62 L. Shen, X. Zhou, C. Zhang, H. Yin, A. Wang and C. Wang, *J. Food Biochem.*, 2019, **43**, e12931.
- 63 K.-T. Li, J.-Y. Li and H.-H. Li, *J. Taiwan Inst. Chem. Eng.*, 2017, **79**, 74–79.
- 64 Z. Xiu, H. Wang, C. Cai, C. Li, L. Yan, C. Wang, W. Li, H. Xin, C. Zhu, Q. Zhang, Q. Liu and L. Ma, *Ind. Eng. Chem. Res.*, 2020, **59**, 9912–9925.
- 65 H. Yin, H. Yin, A. Wang and L. Shen, *J. Ind. Eng. Chem.*, 2018, **57**, 226–235.
- 66 C. Zhang, T. Wang, X. Liu and Y. Ding, *Chin. J. Catal.*, 2016, **37**, 502–509.
- 67 X. Jin, B. Subramaniam and R. V. Chaudhari, *AIChE J.*, 2016, **62**, 1162–1173.
- 68 M. R. A. Arcanjo, I. J. Jr Silva, E. Rodríguez-Castellón, A. Infantes-Molina and R. S. Vieira, *Catal. Today*, 2017, **279**, 317–326.
- 69 C. Zhang, T. Wang, X. Liu and Y. Ding, *J. Mol. Catal. A: Chem.*, 2016, **424**, 91–97.
- 70 B. Sever and M. Yildiz, *React. Kinet., Mech. Catal.*, 2020, **130**, 863–874.
- 71 K.-T. Li and H.-H. Li, *Appl. Biochem. Biotechnol.*, 2020, **191**, 125–134.
- 72 P. P. Pescarmona, K. P. F. Janssen, C. Delaet, C. Stroobants, K. Houthoofd, A. Philippaerts, C. De Jonghe, J. S. Paul, P. A. Jacobs and B. F. Sels, *Green Chem.*, 2010, **12**, 1083–1089.
- 73 J. Xu, H. Zhang, Y. Zhao, B. Yu, S. Chen, Y. Li, L. Hao and Z. Liu, *Green Chem.*, 2013, **15**, 1520–1525.
- 74 H. J. Cho, C.-C. Chang and W. Fan, *Green Chem.*, 2014, **16**, 3428–3433.
- 75 Y.-D. Long, F. Guo, Z. Fang, X.-F. Tian, L.-Q. Jiang and F. Zhang, *Bioresour. Technol.*, 2011, **102**, 6884–6886.
- 76 R. K. P. Purushothaman, J. van Haveren, A. Mayoral, I. Melián-Cabrera and H. J. Heeres, *Top. Catal.*, 2014, **57**, 1445–1453.
- 77 M. Tao, X. Yi, I. Delidovich, R. Palkovits, J. Shi and X. Wang, *ChemSusChem*, 2015, **8**, 4195–4201.
- 78 M. Tao, D. Zhang, X. Deng, X. Li, J. Shi and X. Wang, *Chem. Commun.*, 2016, **52**, 3332–3335.
- 79 M. Tao, D. Zhang, H. Guan, G. Huang and X. Wang, *Sci. Rep.*, 2016, **6**, 29840.
- 80 M. Tao, N. Sun, Y. Li, S. Wang and X. Wang, *Catal. Sci. Technol.*, 2020, **10**, 207–214.
- 81 M. Tao, N. Sun, Y. Li, T. Tong, M. Wielicako, S. Wang and X. Wang, *J. Mater. Chem. A*, 2017, **5**, 8325–8333.
- 82 S. Feng, K. Takahashi, H. Miura and T. Shishido, *Fuel Process. Technol.*, 2020, **197**, e106202.
- 83 H. Kishida, F. Jin, Z. Zhou, T. Moriya and H. Enomoto, *Chem. Lett.*, 2005, **34**, 1560–1561.
- 84 J. Buckingham, F. Macdonald, *Dictionary of Organic Compounds*, Chapman Hall, 6th edn, 1995, vol. 4.
- 85 F. Jin, Z. Zhou, H. Enomoto, T. Moriya and H. Higashijima, *Chem. Lett.*, 2004, **33**, 126–127.
- 86 S. Hoops, S. Sahle, R. Gauges, C. Lee, J. Pahle, N. Simus, M. Singhal, L. Xu, P. Mendes and U. Kummer, *Bioinformatics*, 2006, **22**, 3067–3074.
- 87 S. A. Zavrzhnova, A. L. Esipovicha, S. M. Danova, S. Y. Zlobina and A. S. Belousov, *Kinet. Catal.*, 2018, **59**, 459–471.
- 88 F. Auneau, L. S. Arani, M. Besson, L. Djakovitch, C. Michel, F. Delbecq, P. Sautet and C. Pinel, *Top. Catal.*, 2012, **55**, 474–479.



## Review

- 89 C. B. Rasrendra, B. A. Fachri, I. G. B. N. Makertihartha, S. Adisasmito and H. J. Heeres, *ChemSusChem*, 2011, **4**, 768–777.
- 90 C. Crotti, J. Kašpar and E. Farnetti, *Green Chem.*, 2010, **12**, 1295.
- 91 R. A. Sheldon, *Chem. Commun.*, 2008, 3352–3365.
- 92 S. Özkar, *Int. J. Hydrogen Energy*, 2021, **46**, 21383–21400.
- 93 S. Akbayrak and S. Özkar, *J. Colloid Interface Sci.*, 2021, **596**, 100–107.
- 94 S. Özkar, *Dalton Trans.*, 2021, **50**, 12349–12364.
- 95 S. Akbayrak and S. Özkar, *ACS Appl. Mater. Interfaces*, 2021, **13**, 34341–34348.

